AD NUMBER
AD917474
LIMITATION CHANGES
TO: **Approved for public release; distribution is unlimited.**
FROM: **Distribution authorized to U.S. Gov't. agencies only; Test and Evaluation; 14 MAR 1974. Other requests shall be referred to Night Vision Laboratory, Fort Belvoir, VA 22060.**
AUTHORITY
USAEC ltr, 12 Apr 1974

No. 4

AD

PHOTOEMISSION IN THE 1-2 MICRON RANGE

FINAL REPORT

J. S. ESCHER

1973 December

SPONSORED BY
ADVANCED RESEARCH PROJECTS AGENCY
ARPA ORDER NO. 2182

NIGHT VISION LABORATORY
U.S ARMY ELECTRONICS COMMAND
FORT BELVOIR, VA. 22060

CONTRACT NO. DAAK02-72-C-0412

RCA ELECTRONIC COMPONENTS
DAVID SARNOFF RESEARCH CENTER
PRINCETON, NEW JERSEY 08540

DISTRIBUTION STATEMENT

[redacted]

the Director, Night Vision Laboratory, Fort Belvoir, Virginia 22060.

Report No. 4

FINAL REPORT

1972 April 17 - 1973 October 16

PHOTOEMISSION IN THE 1-2 MICRON RANGE

Contract No. DAAK02-72-C-0412
ARPA Order No. 2182
Program Code No. 2D10

Effective date: 1972 April 17
Expiration date: 1973 October 16
Amount of Contract: $267, 511.

Principal Investigator: John S. Escher
Phone Number: 609-452-2700, Ext. 2560

Report prepared by:

J. S. Escher
Electro-Optics Laboratory
RCA Electronic Components

Sponsored by

NIGHT VISION LABORATORY
U.S. ARMY ELECTRONICS COMMAND
Fort Belvoir, Va. 22060

and

ADVANCED RESEARCH PROJECTS AGENCY
Washington, D. C. 20301

1973 December 6

RCA ELECTRONIC COMPONENTS
David Sarnoff Research Center
Princeton, New Jersey 08540

SUMMARY

Work under this contract has focused on a field-assisted 1-2 micron-sensitive photoemitter with a reverse biased Ge p-n junction and a thin Cs-O-activated emitting layer of negative electron affinity (NEA) GaAs. The p^+-GaAs provides an effective single-crystal low-work-function large-area biasing contact for the Ge p-n junction and allows the n-Ge to be sufficiently thin for optimal performance. Calculations show that some cooling, perhaps to -80°C, will be necessary to reduce the dark current well below the signal level. More detailed theoretical calculations (than those reported in Quarterly Report No. 1) are presented which show that 1-4% quantum efficiency in transmission is possible from either a GaAs/Ge or an InP/Ge device. The optimal design parameters are calculated, and the sensitivity of the parameters is discussed. GaAs/Ge growth using the metal chloride and organometallic vapor phase epitaxy (OM-VPE) methods has been studied in some detail. Only the OM-VPE process results in a true p-GaAs/n-Ge heterojunction essential for our device. The metal chloride process suffers from Ge autodoping into the initial GaAs growth layer. Vacuum activation levels of thick GaAs/Ge have been very high in the reflection mode - comparable to homojunction GaAs/GaAs activation levels. Ultra-thin diffused Ge junctions (less than 1000 Å deep) have been successfully fabricated using the OM-VPE method. Furthermore, negative electron affinity has been achieved on samples as thin as 0.15 micron of GaAs grown on Ge by OM-VPE. These results coupled with photovoltaic and electroluminescent measurements indicate that GaAs/Ge grown by OM-VPE should be suitable for the 1-2 micron device. Significant progress toward demonstrating the feasibility of this device has been prevented during the last six months of the contract by the failure of both mesa and planar-type diodes to survive even moderate heat-cleaning cycles in vacuum. Probable breakdown mechanisms are discussed, and possible "fixes" are mentioned. Because of the diode breakdown problem, field-assisted photoemission experiments have not been possible.

FOREWORD

Contract No.:	DAAK02-72-C-0412 ARPA Order No. 2182
Contractor:	RCA Corporation
Date of Contract:	1972 April 17
Amount of Contract:	$267,511.
Completion Date:	1973 October 16
Title of Project:	Photoemission in the 1-2 Micron Range
Project Engineer:	John S. Escher Telephone: 609-452-2700, Ext. 2560
Report prepared by:	J. S. Escher Electro-Optics Laboratory RCA Electronic Components
Work done by:	J. S. Escher C. C. Wang G. H. Olsen J. P. Carroll
Report approved by:	A. H. Sommer, Acting Manager Electro-Optics Laboratory

The research in this report was carried out in the Electro-Optics Laboratory, RCA Electronic Components, under the direction of Dr. B. F. Williams, Manager, Electro-Optics Laboratory, in the Materials Research Laboratory, RCA Laboratories, under the direction of Dr. J. J. Tietjen, Director, and in the Process and Applied Research Laboratory, RCA Laboratories under the direction of Dr. P. Rappaport, Director. Key research personnel include Dr. J. S. Escher, Project Engineer, Dr. C. C. Wang, and Dr. G. H. Olsen. This report covers the period 1972 April 17 - 1973 October 16.

TABLE OF CONTENTS

LIST OF FIGURES

Figure | page

Appendix

I. INTRODUCTION

The research conducted under this contract was directed toward developing a photoemitter with high quantum efficiency to 1-2 micron radiation and with low dark current. Calculations presented here, coupled with encouraging experimental results, indicate that a 1-2 micron-sensitive photoemitter is feasible. Our device is a Ge p-n junction field-assisted photoemitter utilizing a single-crystal negative electron affinity (NEA) emitter for a large-area biasing contact. Calculations discussed in detail in the Appendix show that a transmission quantum efficiency of 1-4% at 1.55 μm and -80°C should be obtainable with either a GaAs/Ce or an InP/Ge device. Field enhanced photoemission into vacuum has not been measured because of diode breakdown problems.

II. TECHNICAL DISCUSSION

A. The Electron Transparent Contact and the GaAs/Ge Device

Recent years have seen a great deal of work on negative electron affinity activated III-V materials and silicon to achieve higher quantum efficiencies and longer wavelength response.[1,2] Present theories of activation and experimental results strongly suggest that quantum efficiencies of .1% or greater from a non-field-assisted photoemitting device for wavelengths much greater than 1.2 microns will be practically impossible.[3,4] Previous photoemitter devices designed for greater than one-micron sensitivity have suffered from such limitations as very low quantum efficiency (less than 10^{-4}), high dark current (thermionic emission at room temperature), and non-reproducible results.

Two promising design types are the reverse biased p-n junction emitter and the tunneling emitter. The reverse biased junction emitter is basically a hot electron emitter. Problems with this device are that, if a metal film is used to make large-area electrical contact on the emitting surface, the photoexcited hot electrons are severely attenuated in the metal film before reaching the metal-vacuum interface. If, however, the surface n-region is made thicker and thereby becomes the electrical contact, the photoexcited electrons are again severely attenuated in the long flat-band n-region.[5] Tunneling emitter designs have suffered from high-field breakdown in the insulator region and poor quality (poor minority carrier diffusion length) of the emitting layer.[6] A completely thermalized emitter design with field-assisted biasing has been proposed by several workers recently.[7] The severe problem faced by most such designs, however, is that ideal heterojunctions must be grown. The heterojunction interface must not have even a few kT barrier in the conduction band, otherwise, photoexcited electrons will be trapped and lost.

The bulk of our program was based on a $GaAs(p^+)/Ge(n^+)/Ge(p^+)$ field-assisted hot electron device which offers the possibility of relatively high

sensitivity out to the band gap of Ge, approximately 1.8 microns. The GaAs surface is activated with Cs-O to achieve NEA. An electron energy band diagram for this device is shown in Fig. 1. The presence of the GaAs allows the n-Ge region to be sufficiently thin (on the order of a few hundred Angstroms). The highly-doped GaAs (approximately $1x10^{19}/cm^3$ Zn) is sufficiently thick to provide an effective large-area electrical contact for biasing the Ge p-n junction. The Ge p-n junction is reverse biased in operation. Tunneling will most likely set the upper limit of the dc bias applied to the Ge junction since, to optimize performance, the p-Ge substrate should be $\sim 1x10^{18}/cm^3$ (see Appendix).

Because of the excellent lattice match (GaAs, 5.654 Å vs Ge, 5.658 Å) and coefficient of thermal expansion match between GaAs and Ge,[8] the quality of the GaAs should be sufficiently good so that photoexcited electrons reaching the GaAs will have a reasonable probability of diffusing to the GaAs surface and being emitted. Hence, the GaAs acts as an electron transparent contact for this device and is designed to avoid the problems faced by previous reverse-biased p-n junction emitters. The n-Ge region is formed by As diffusion into the p-Ge wafer and provides the needed blocking barrier for holes. For incident light of wavelength greater than about 0.9 micron, the GaAs becomes optically transparent (except for reflection losses at the GaAs vacuum interface, 32%, and at the GaAs-Ge interface, $\simeq$.4%). Light of wavelengths greater than 0.9 micron then travels into the Ge where it photoexcites electron-hole pairs. Photoexcited electrons in the p-Ge diffuse to the depletion region of the reverse-biased p-n junction where the field sweeps them into the GaAs and finally into vacuum. Hence, this device should have a very broad band sensitivity in the reflection mode from the cut-off wavelength of the vacuum window used for the device to the band-gap-limited emission of the Ge. Clearly, the device can be made to operate in the transmission mode by thinning a window in the p-Ge.

B. The Electron Transparent Contact and the Differential Grade Device

The GaAs/Ge device described above is a hot electron emitter; that is, the photoexcited electrons generated in the p-Ge must cross the Ge p-n junction depletion region into the GaAs as "hot carriers." Once the photoexcited carriers reach the GaAs, they may thermalize in the GaAs conduction band and still be emitted into vacuum since they can cross the GaAs by thermal diffusion. The critical question for the GaAs/Ge device is whether the hot electron losses will be low enough to allow reasonably efficient 1-2 μm emission. Calculations discussed in Section II-D and in the Appendix indicate that the thickness W_f of the flat band n-Ge must be $\leq$500 Å to reduce hot electron losses to an acceptable level. We describe in this section another field-assisted device which is capable of 1-2 μm emission that does not require hot electron transport but only thermalized transport.

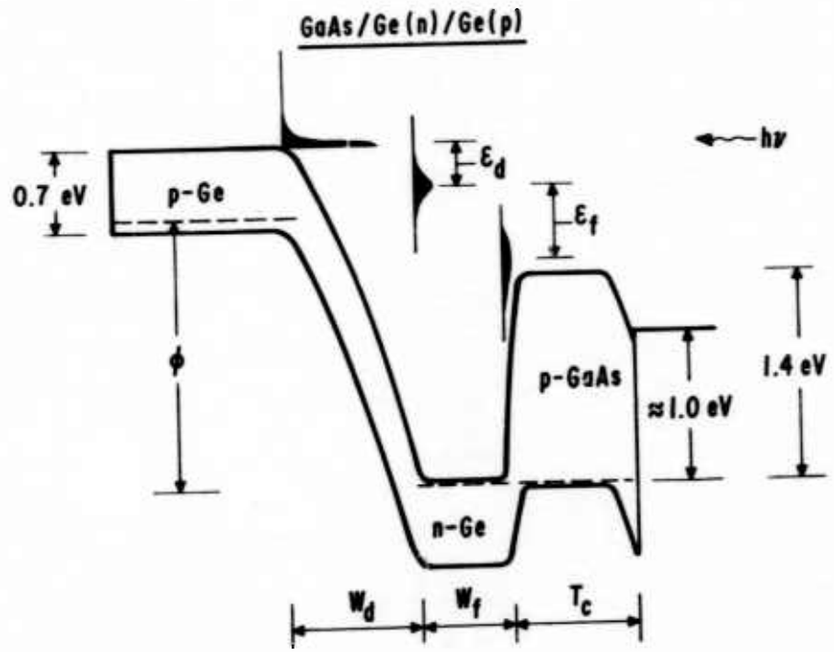

Fig. 1. Energy band diagram for the GaAs/Ge device. ϕ is the applied reverse bias to the junction. W_d is the width of the depletion region. W_f is the width of the flat band n-Ge region. T_c is the thickness of the GaAs. $\mathcal{E}_d$ is the energy lost in the depletion region and $\mathcal{E}_f$ is the energy lost in the flat band region of the Ge.

Figure 2(a) and (b) show the energy band diagram for this device in the unbiased and biased state, respectively. We initially proposed liquid-phase epitaxially grown GaAlSb as the detecting and emitting layers, respectively. The principle of operation of the device does not depend on these particular materials, however. Note that photoexcited electrons generated in the narrow band gap GaAs layer can move by thermal diffusion through the intermediate GaAlSb layer into the NEA GaAlSb layer and into vacuum. As with most heterojunction devices, the interfacial recombination velocity will be a critical parameter in the operation of this device. Also, long electron diffusion lengths are desirable. For both these reasons, liquid-phase epitaxy (LPE) would have the advantage over vapor-phase epitaxial (VPE) growth for this particular device. An important difference between this design and other similar heterojunction thermalized transport devices[7] (see Fig. 3) is the grading of the intermediate layer of our device. The relative injection of holes and electrons into the GaAlSb is controlled by the abruptness of the barrier instead of the relative heights of these barriers. The doping of the intermediate layer is low compared to the emitting or detecting layer so that the applied bias is mostly across this layer. A non-graded structure such as in Fig. 3 requires that, under suitable bias, the barrier for electron injection (B1 in Fig. 3) "go away" under bias before the necessary hole barrier (B2 in Fig. 3) vanishes. Note that there must be no conduction energy band notches of $\geq kT$ in magnitude for this or any completely thermalized emitter design.

A difficult materials question for the graded intermediate layer is whether such a very large degree of band gap grading can be accomplished. To date, we have been able to grow flat-band GaAlSb on GaAs by LPE. Activation results on two GaAlSb samples have been very poor. Because of the severe materials growth problems faced by this design, we did not continue work on the differential grade device.

C. Calculations - Dark Current

In operation, photoexcited electrons in the p-Ge which diffuse and fall into the n-Ge hole without being emitted cause a forward bias of the GaAs/Ge heterojunction. The β of the p-n-p transistor times this current is injected from the GaAs under the hole barrier and crosses into the p-Ge. This current is not observed outside the device. The dark current that is emitted is due to the fraction of electrons thermally excited in the flat-band p-Ge which is able to cross the n-Ge, enter the p-GaAs, and be emitted into vacuum. The thermal generation of electrons in the p-Ge is given by

$$J = \frac{eD_n n_{po}}{L_n} = \frac{eD_n n_i^2}{L_n p_{po}} \quad . \tag{1}$$

J is $\sim 1 \times 10^{-7}$ amp/cm^2 at 25°C using $D_n = 100$ cm^2/sec, $L_n = 10$ μm, $n_i = 2.5 \times 10^{12}$/cm^3, and $p_{po} = 1 \times 10^{18}$/cm^3. The available signal current density (difference between foliage and hard targets [A. D. Schnitzler and J. Malamas, "Image Detection and Air Glow"]) is $\sim 1 \times 10^{-8}$ amp/cm^2 at

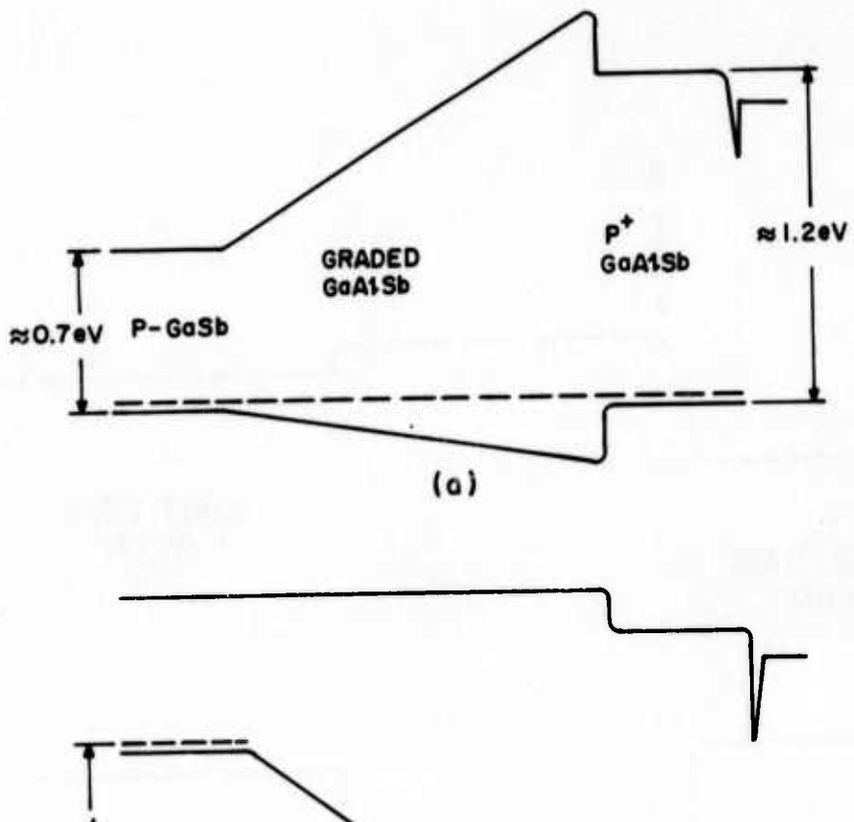

Fig. 2. Differential grade heterojunction emitter

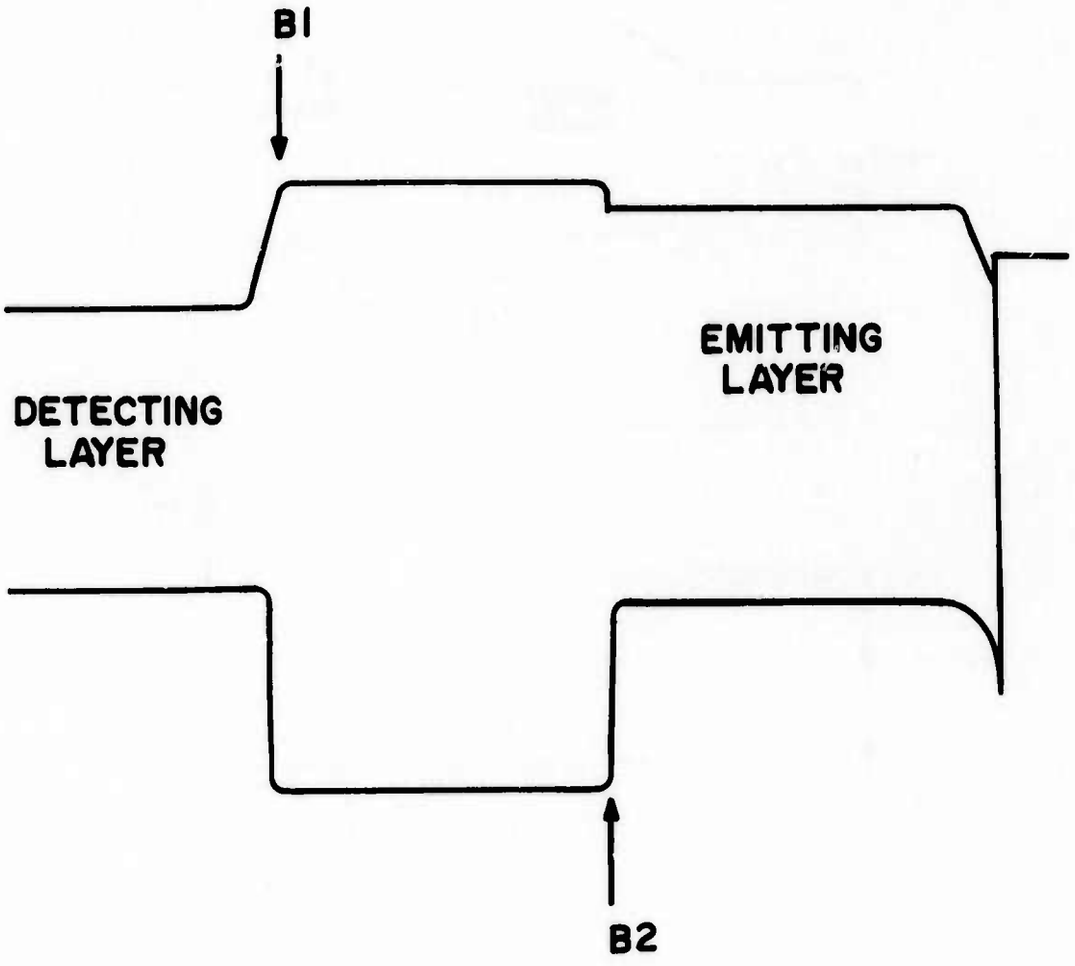

Fig. 3. Thermalized electron emitter with flat-band intermediate layer.

1.55 μm. Assuming f/1.4 optics reduces this level by ∿1:10. Hence, the incident signal level is $\sim 1 \times 10^{-9}$ amp/cm^2. It is clear that some cooling of the device will be necessary. Cooling to -20°C will reduce the generated dark current an order of magnitude below the signal level, but -80°C (dry ice) would be better.

D. Calculations - Quantum Efficiency in Transmission

In this section, we outline the results of calculations made on the expected transmission quantum efficiency for the GaAs/Ge device. The details of the calculation are in the Appendix. The calculated transmission quantum efficiency of the complete device is conveniently broken up into three parts: First, the photoelectron generation and diffusion in the flat-band p-Ge into the p-n junction. Second, the hot electron transport across the p-n junction. Third, the electron injection into the GaAs and diffusion into vacuum. Note that all calculations assume λ = 1.55 m, transmission-mode operation, an effective AR coating on the back, and T = -80°C.

The transmission quantum efficiency of just the flat-band p-Ge is quite good. Assuming an electron diffusion length of 10 μm and a back surface recombination velocity ratio of 1.0 (i.e., S divided by the diffusion velocity of L/τ) gives a 70% transmission quantum efficiency into the p-n junction at 1.55 μm. The otpimal germanium thickness for the above conditions is ∿3.5 μm, although increasing this thickness to 10 μm only reduces the transmission efficiency by 45%. (See Figs. 1A and 2A of the Appendix.) The above calculation was performed using the usual thermalized electron diffusion equation and should be a realistic estimate of the actual efficiency from this part of the device.

Next, we consider the efficiency of the p-n junction region where the electrons are now "hot". The theoretical model used here is that of D. J. Bartelink, et al.,[9] appropriately modified for our case of no impact ionization. That is, we will restrict the reverse bias on our junction such that avalanching does not occur. Results of these calculations (see Appendix, Figs. 3A-8A) show two important facts. First, we want highly doped p-Ge to minimize the electron losses in the depletion width of the biased junction. The limit on p-type doping is given by the fact that we need an ∿1.5-2.0 volt breakdown voltage, and $>10^{18}$/cm^3 will break down due to tunneling before this level of bias. The second fact is that we need to minimize the width of the flat-band n-Ge region. This region, ideally, must be 500 Å or less. Assuming 1×10^{18}/cm^3 p-Ge, a 1.6 volt bias, 250 Å n-Ge region, 85 Å hot-electron mean free path, .037 eV energy loss per collision to optical phonons, and T = -80°C gives a total transmission probability across the junction (including quantum mechanical reflections at the n-Ge/p$^+$GaAs interface) of 40%. There are many more approximations in this calculation than in a thermalized transport calculation. However, we have tried to use the best data available and to make reasonable approximations where necessary.

The final stage is the NEA emitter itself. Again, the calculation is based on the thermalized diffusion equation. We have assumed infinite back surface recombination at the n-Ge/p-GaAs interface. The appropriate absorption coefficient α to use is approximated by the following. There will be $\sim$0.3 to 0.4 eV (above GaAs conduction band) hot electrons entering the GaAs. The mean penetration depth or range for these hot electrons can be estimated by using the random walk equation

$$R = \lambda_p \sqrt{N} \tag{2}$$

where λ_p = 85 Å is the mean distance between collisions and N is the number of collisions before thermalizing. Since .037 eV is lost per collision, $N \sim 10$. Hence $R \sim 250$ Å, and, for $L >> R$, $\alpha \approx 1/R = 40$/micron. Using this value of α and L = 1.0 μm gives an optimal transmission quantum efficiency of $\sim$30% for a GaAs thickness of 500 Å. Increasing the GaAs thickness to 0.1 micron only reduces this efficiency to $\sim$20%. Assuming an NEA surface escape probability of 25-50% gives a total emitted transmission quantum efficiency through the GaAs of 5-15%.

The complete transmission quantum efficiency of the entire device is then estimated to be

$$QE_T \approx (0.7)(0.40)(.05\text{-}.15)$$
$$QE_T \sim 1\text{-}4\% \text{ at } 1.55\ \mu m \ . \tag{3}$$

The above calculation has been repeated for the case of NEA InP/Ge. Within the uncertainties stated above, the result is slightly better since InP has a 0.1 eV lower band gap. The lattice match (5.869 vs 5.657 Å) is much worse than that of GaAs/Ge; however, as long as L(InP) >> Range(InP), the over-all transmission efficiency will not be significantly reduced. (See Fig. 9A in the Appendix.) However, such a large lattice mismatch, 3.7%, may lead to high reconbination due to a large number of interface states.[10]

E. Epitaxial Growth of GaAs on Ge

One of the main objectives and accomplishments of this contract has been to determine the optimal conditions for the growth of high quality single-crystal thin films of p-GaAs on Ge within the requirements of Zn-doping concentration and minimal As diffusion into the Ge. In this section, we describe some of the growth experiments that we have made to achieve our objective for the GaAs/Ge device.

During the course of this study, we found very early that substrate preparation of the Ge plays an important role in determining the quality of the resulting epitaxial film. The best results to date have been obtained using Ge substrates which are both mechanically and chemically polished. After mechanical polishing, the wafers are first etched with

CP4 to remove work damage from the mechanical polishing treatment. Then the wafers are chemically polished with a quso+H_2O+sodium hydroxide+H_2O_2 solution using a pix pad. The wafers are then cleaned thoroughly with TCE in order to remove any traces of wax remaining after demounting from the polishing block. This was followed by an ultrasonic cleaning to remove any small particles of the polishing pad which may have remained from the chemical polishing treatment. Finally, the wafers are vapor etched for 3-5 minutes in a HCl+H_2 atmosphere (1:30 dilution) at a temperature of approximately 825°C, thereby providing a clean oxide-free surface on which to deposite the GaAs film.

1. Metal Chloride Vapor-Phase Epitaxy

The meltal chloride vapor-phase (MC-VPE) growth system was used initially to prepare GaAs/Ge films for this contract. The growth system is identical to that previously described by Tietjen and Amick[11] in which GaCl combines with As vapor to form GaAs via the reaction

$$2\ GaCl + \tfrac{1}{2}As_4 + H_2 \rightleftharpoons 2GaAs + 2HCl \quad . \qquad (4)$$

The GaCl is formed by passing HCl over a heated quartz boat containing Ga whereas the As vapor is formed as a result of the thermal decomposition of the AsH_3. The GaAs films are doped p-type by introducing Zn vapor into the system during growth. This is accomplished by passing H_2 over a heated quartz bucket containing the metal. The doping level is controlled simply by raising or lowering the bucket temperature. Note that HCl is an active by-product of this growth process. As a result, GaAs films less than approximately 0.5 micron thick suffered severely from autodoping effects of Ge.[12] The Ge acts as an n-type dopant and more than compensates the $10^{19}/cm^3$ Zn doping concentration for thin films. The autodoping problem, being a fundamental problem with this growth system, has led us to employ the organometallic vapor-phase (OM-VPE) growth method during the remainder of this contract.

2. Organometallic Vapor-Phase Epitaxy

The OM-VPE growth process[13] has two important advantages for our device over the MC-VPE process described above. First, the OM-VPE process has no active by-products such as HCl which might lead to autodoping problems noted with MC-VPE of GaAs/Ge. Second, the usual GaAs growth temperature for the OM-VPE process is 100-150°C lower than that for the MC-VPE process. The lower growth temperature results in thinner diffused junctions in the Ge than does the MC-VPE process. (See Section G.) Essentially no NEA activation results were available on OM-VPE GaAs before this contract. There had been some concern that GaAs grown by this process may suffer from carbon contamination and thereby not yield high activation levels.[14] This worry proved to be unfounded, and excellent activation results have been achieved on GaAs/GaAs and GaAs/Ge grown by OM-VPE. (See Section F.)

F. GaAs/Ge Activation

Because of the excellent lattice match and thermal expansion match between GaAs and Ge, the quality of GaAs grown on Ge should be very good. These expectations have been confirmed by generally high activation levels from the GaAs. Except for the thin GaAs/Ge (under 0.5 micron) samples grown by MC-VPE, GaAs/Ge activation levels are within experimental variability as good as typical GaAs/GaAs activation levels.

Table I shows the results to date on NEA activation levels obtained on GaAs/GaAs and GaAs/Ge grown by different processes. Maximum and typical activation levels are indicated where sufficient statistics are available. Note that all results are for reflection-mode (i.e., light incident on the same surface as that from which electrons are emitted) and that the activations were performed in an all-metal ultrahigh vacuum system. Furthermore, all values have been corrected for the optical absorption of glass (10%).

There are two general results to be noted. First, for the thick samples tested, the GaAs/Ge results for both MC-VPE and OM-VPE are quite good. Considering the fact that so few (less than six) such samples of each have been activated, we feel that these activation levels are satisfactory. The second general result is that involving thin samples. GaAs/Ge grown by MC-VPE most likely suffers from autodoping of the grown epitaxial by Ge due to the active by-product, HCl.[12] The autodoping effect of Ge heavily compensates the p^+-GaAs making activation to NEA impossible. Similarly grown thin samples, grown by OM-VPE, do not appear to suffer from this problem. This latter result is particularly important for our device. The ability to achieve NEA on very thin GaAs/Ge grown by OM-VPE coupled with reduced diffusion of As into the p-Ge substrate (see Section G) makes this growth process most suitable for our device.

Analysis of thin GaAs films activated to NEA is complicated by the fact that the diffusion length is now equal to or greater than the cathode thickness. Fig. 4 shows the calculated available white-light sensitivity (surface escape probability assumed equal to unity) from GaAs as a function of the cathode thickness from 0.0 to 0.5 micron thick and for 0.1 to 5.0 micron diffusion lengths. Note that the available sensitivity is independent of diffusion length for $L \geq 0.5$ micron. If we assume $L \geq 0.5$ micron, then the 250 to 475 μA/lm activation levels from the 0.15 and 0.30 μm thick cathodes correspond to a surface escape probability of approximately 45%. Analysis of yield shapes near threshold cannot give a good estimate of diffusion length or cathode thickness. This fact is evident in Figs. 5 and 6 which show theoretical yield curve shapes for different cathode thicknesses and cathode diffusion lengths. Fig. 7 shows, however, that the yeield curve shape near threshold for thin GaAs depends strongly on doping - i.e., the optical absorption coefficients used. The absorption data used to generate the yield curve shapes in Fig. 7 were taken from Kudman and Seidel.[15] Fig. 8 is a best fit for the thin, 0.3 micron, GaAs/Ge sample grown by OM-VPE which activated to 475 μA/lm. The best

TABLE I

GaAs/GaAs and GaAs/Ge Activations

GaAs/substrate, process, thickness	Maximum μA/lm	Typical μA/lm
GaAs/GaAs MC-VPE, thick >5. μm	1700	1300
GaAs/GaAs LPE, thick	1550	1200
GaAs/GaAs OM-VPE, thick	1475	
GaAs/Ge MC-VPE, thick	1475	
GaAs/Ge OM-VPE, thick	1375	
GaAs/Ge MC-VPE, thin 1.0 μm	1000	
GaAs/GaAs MC-VPE, thin 0.3 μm	420	
GaAs/Ge MC-VPE, thin 0.3 μm	35	
GaAs/Ge OM-VPE, thin 0.3 μm	475	
GaAs/Ge OM-VPE, thin 0.15 μm	250	

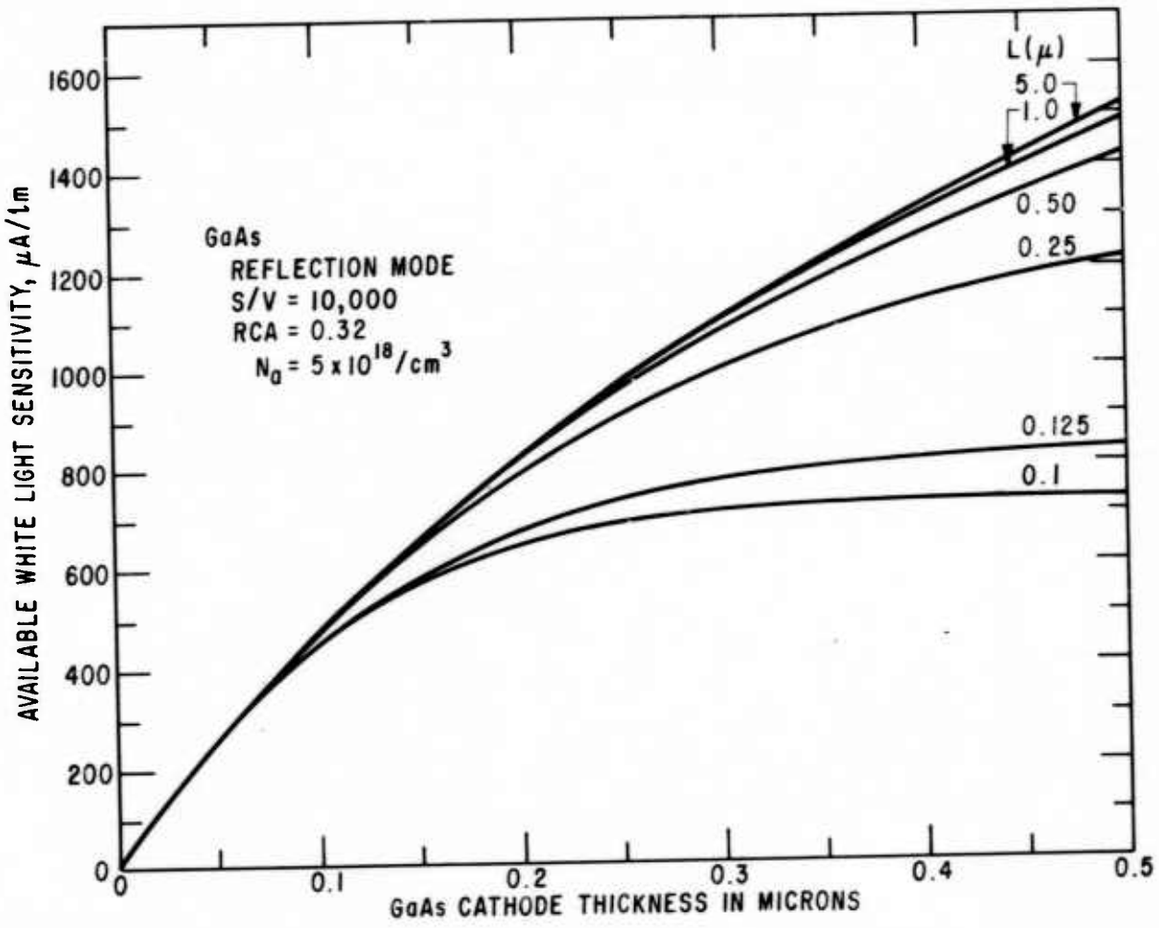

Fig. 4. Calculated available white-light sensitivity (in μA/lm) from NEA GaAs. The surface escape probability is taken to be 100%, the back surface recombination velocity is taken to be infinite. The GaAs cathode thickness is varied from 0.0 to 0.5 μm while the diffusion length is varied from 0.1 to 5.0 μm.

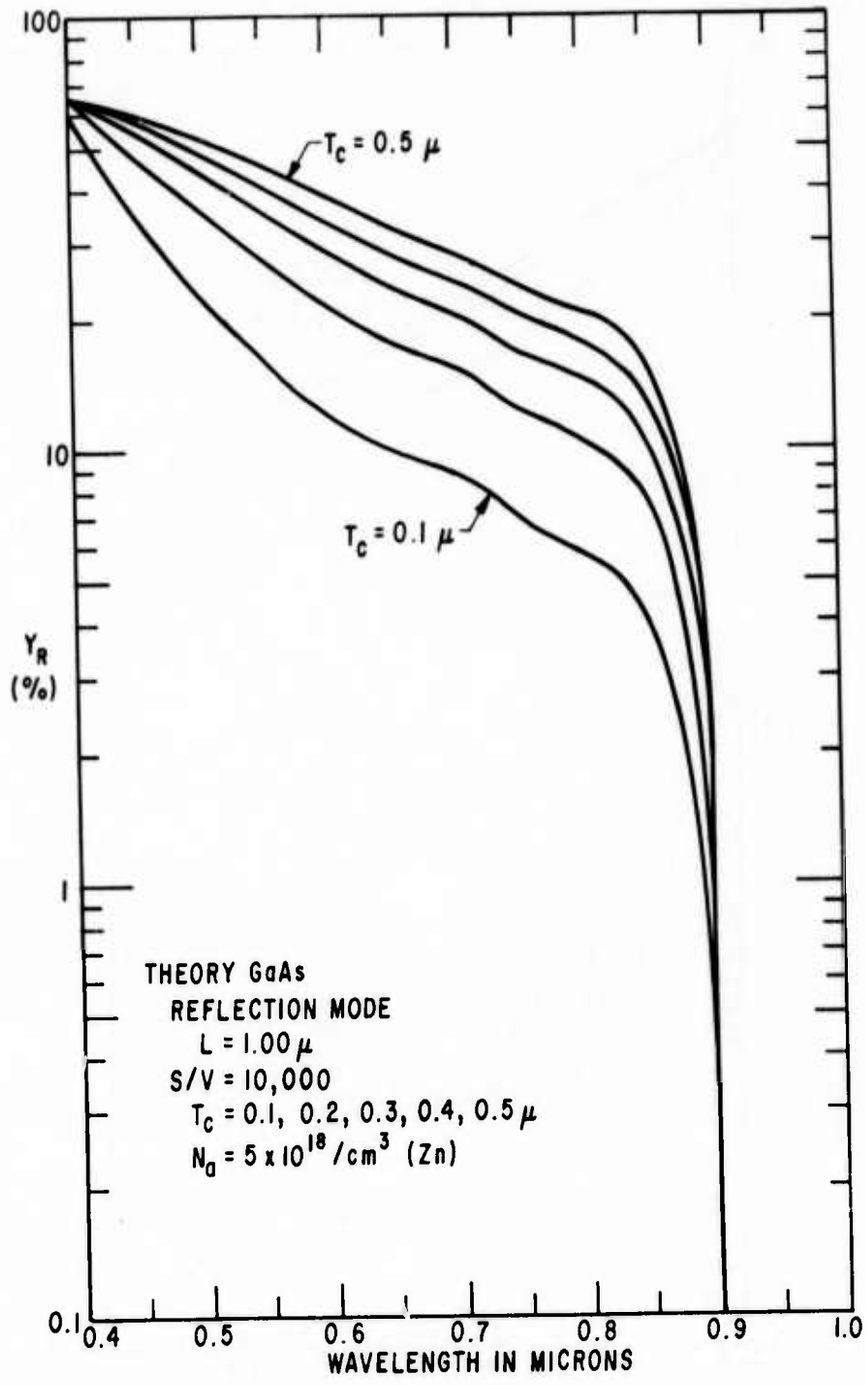

Fig. 5. Calculated quantum yield curve for NEA GaAs. Diffusion Length L is 1.0 μm and the back surface recombination velocity (GaAs/Ge interface) is taken to be infinite. The curves shown are for 0.1 through 0.5 μm cathode thickness T_C. Escape probability is 100%.

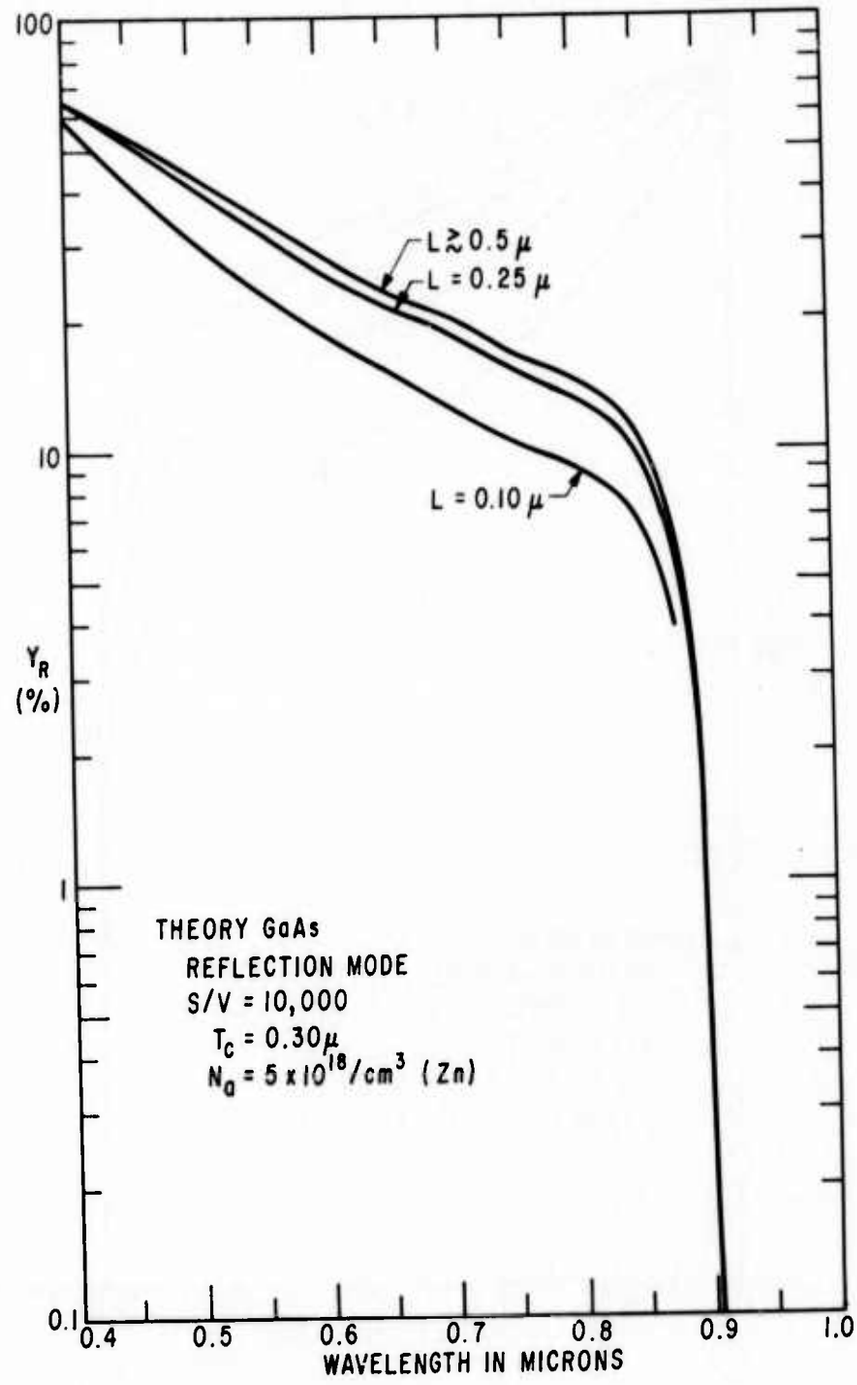

Fig. 6. Calculated quantum yield curve for NEA GaAs. Cathode thickness T_c is taken as 0.3 μm and the back surface recombination velocity is infinite. Diffusion length L is varied from 0.1 to ≳0.5 μm. Escape probability is 100%.

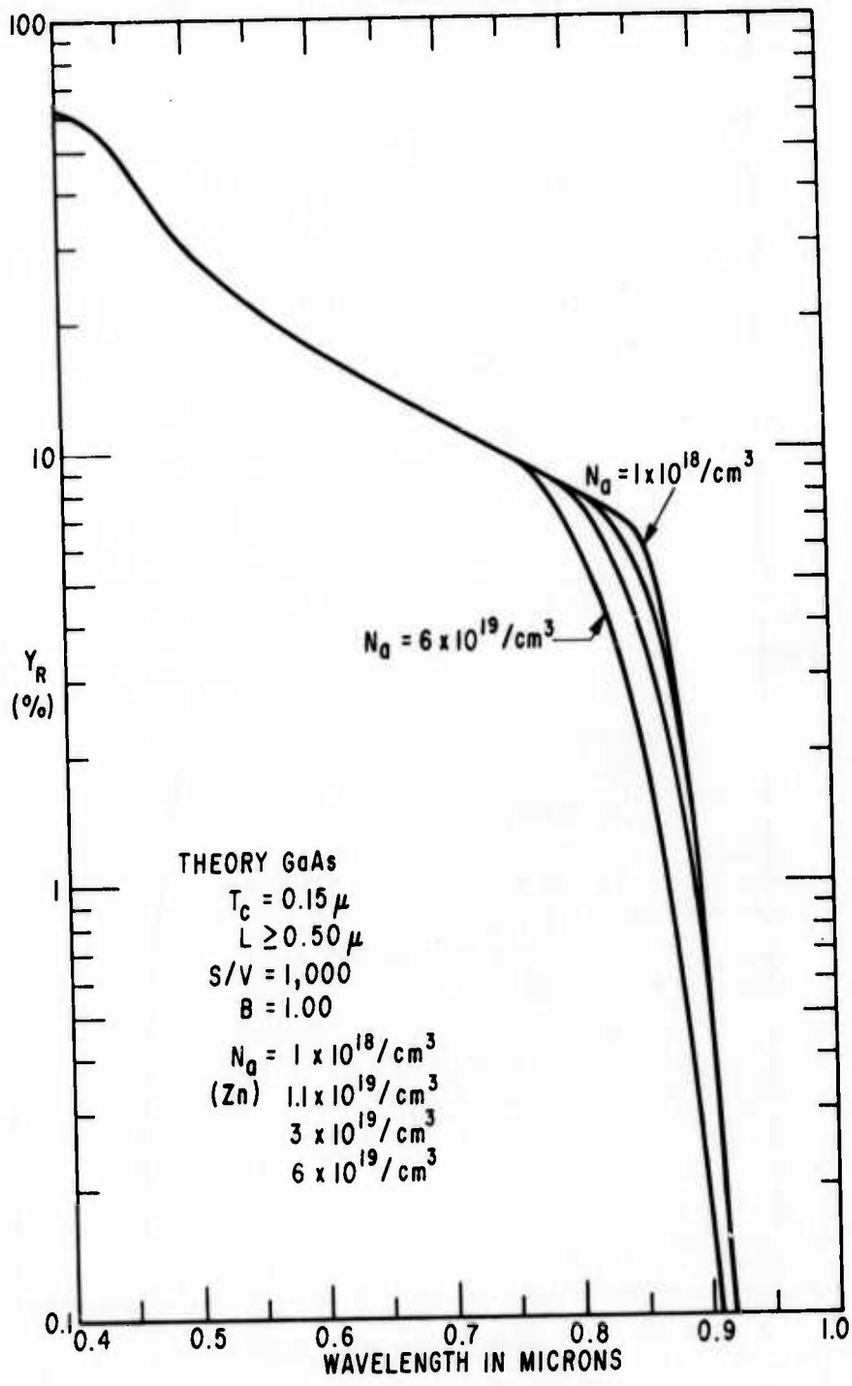

Fig. 7. Calculated quantum yield curve for NEA GaAs. Cathode thickness T_c is 0.15 μm, diffusion length L is ≥0.50 μm, back surface recombination velocity is infinite, and the escape probability is 100%. The Zn doping concentration is varied from $1 \times 10^{18}/cm^3$ to $6 \times 10^{19}/cm^3$.

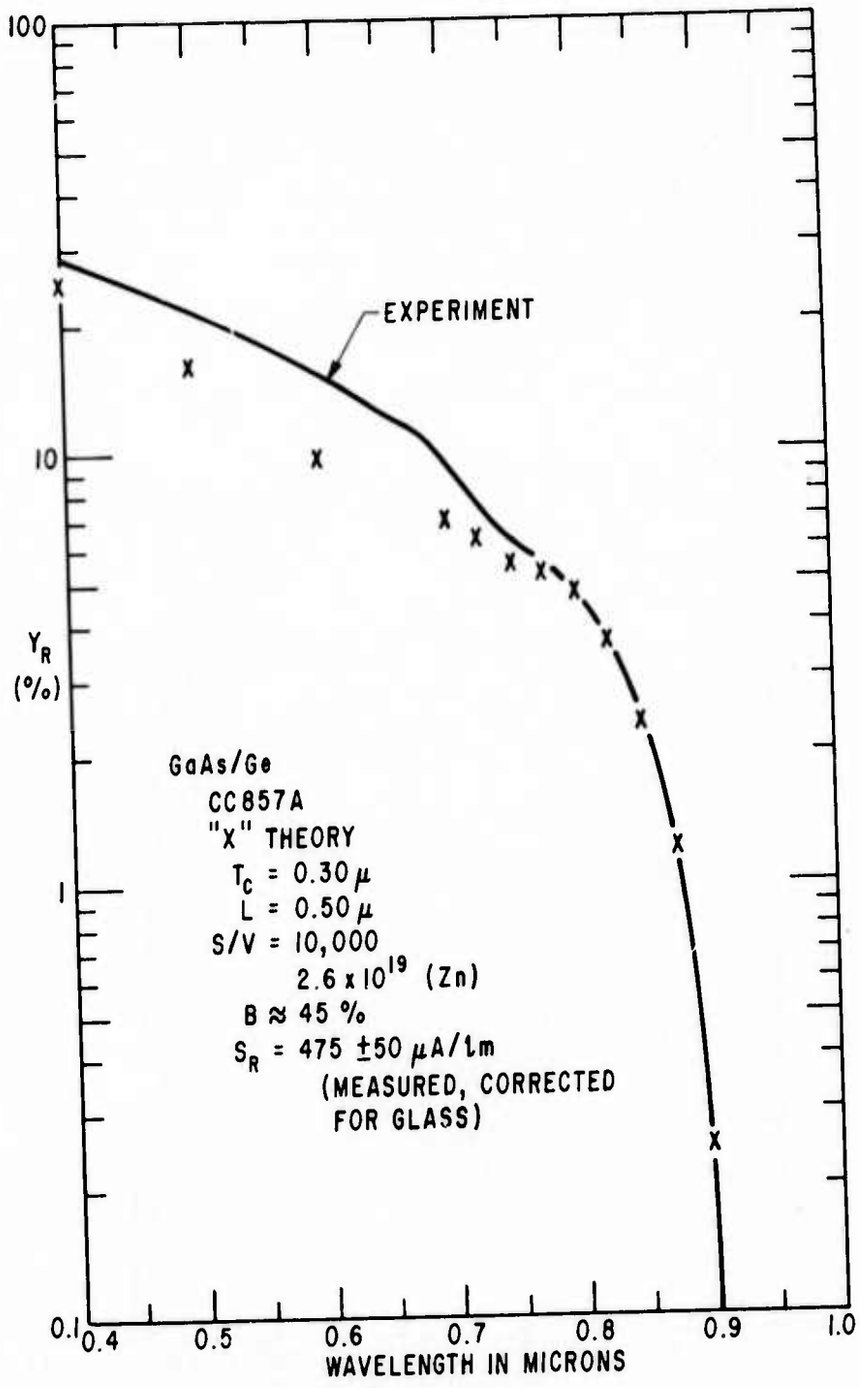

Fig. 8. Calculated and experimental NEA GaAs quantum yield curves. The best fit calculated curve is for T_c = 0.30 μm, L = 0.50 μm, and a surface escape probability of ≈45%.

fit is obtained for a $2.6 \times 10^{19}/cm^3$ doping concentration while the estimates for the diffusion length and surface escape probability are only reasonable guesses. The doping concentration estimated from the yield curve fit, however, is consistent with the doping concentration measured by the IR plasma resonance technique.[16]

G. P-N Junction Formation in Ge

Formation of the p-n junction in Ge is probably the most critical and difficult step in the fabrication of this device. Calculations discussed in Section D and in the Appendix indicate that the depth of the n-Ge layer must be $\sim$500 Å for successful operation. The achievement of such thin diffused junctions is difficult but has been accomplished with both As and P diffusions. This has been the goal of much of our effort on this contract.

In practice, the p-Ge wafer is exposed to As during the growth of the GaAs. All the variables of the GaAs growth such as growth temperature, growth time, condition of the substrate, etc. affect the depth and nature of the As diffusion into the Ge. For our requirement of a very thin diffused layer, it is not necessary to deliberately make a p-n junction in the Ge by diffusion or ion implantation before the GaAs growth. The process of growing GaAs/Ge results automatically in a diffused n-Ge layer just below the grown epitaxial GaAs layer. Hence, our experimental work has been aimed at varying the GaAs growth conditions in such a way as to systematically determine the proper growth conditions for high quality GaAs and sufficiently thin n-Ge junctions.

The arsenic diffusion into the p-Ge can be simply described by the one-dimensional diffusion equation for atomic diffusion,

$$\frac{\partial C(x,t)}{\partial t} = D(T) \frac{\partial^2 C(x,t)}{\partial x^2} \quad , \tag{5}$$

where C is the impurity concentration and D(T) the diffusion coefficient for As into Ge at temperature T.[17] Taking the boundary condition of "constant surface concentration" of concentration C_s, the solution to Eq. (5) is given by

$$C(x,t) = C_s \operatorname{erfc}(x/2\sqrt{Dt}) \tag{6}$$

where x is the distance below the surface and t is the time of diffusion. Taking the p-n junction boundary as seen in an angle lap staining technique to be when $C/C_s \approx 0.1$, Eq. (6) can be solved to give an expression for the depth of diffusion versus time of diffusion given approximately by

$$X(T,t) \approx 3\sqrt{D(T)t} \quad . \tag{7}$$

The diffusion constant varies over a limited temperature range as

$$D(T) = D_o e^{-\Delta E/kT} \tag{8}$$

where D_o is the diffusion coefficient extrapolated to infinite temperature and ΔE is the activation energy of diffusion. (See, for example, Ref. 17, p. 29.) Hence, we have, for a constant diffusion time,

$$X^2 \propto D(T) \propto e^{-\Delta E/kT} \tag{9}$$

$$\log X^2 \propto -\Delta T/kT \tag{10}$$

$$\therefore \log X \propto 1/T \quad . \tag{11}$$

We have employed the angle lap staining technique extensively throughout this contract as a method of determining the thickness of the GaAs growth and the depth of the As diffusion into the p-Ge wafer. A 5° angle block was used, and an n-type stain (465 ml H_2O + 57.5 g $CuSO_4$ + 50 ml HF + light) was applied to show the depth of the As diffusion. A magnification of 1000X allowed junction depths to be measured down to approximately 1000 Å. Occasionally the n-type stain fails to stain or it stains only partially. This situation can cause confusion, and therefore the procedure should ideally be repeated at least once.

One of the first experiments performed was a test of Eq. (7). A series of MC-VPE GaAs/Ge samples was made in which the Ge wafer was first exposed to As at 800°C for various times, and then a thin GaAs epitaxial layer was grown. The thin GaAs layer (1-2 microns) makes the angle lap and staining measurements much easier. The thickness of the n-Ge stands out as a dark band between the lighter p-Ge and p-GaAs layers. Fig. 9 is a typical example of a 5° angle lap and n-stain using 500X. Using this measurement technique, we have generated the data for Fig. 10. The time axis in Fig. 10 represents the exposure time of the p-Ge wafer to As prior to the GaAs growth. Note that the time for the GaAs growth is only 1-2 minutes, and therefore the additional As diffusion which occurs during growth is negligible except for the shortest diffusion times, samples #7-6-72:4 and #5-24-72:3. Also shown in Fig. 10 are three theoretical curves using Eq. (7) for $D = 1.5 \pm .5 \times 10^{-3}$ $\mu m^2/sec$. The fit to the data is reasonably good, and the range of values for the diffusion coefficient of As into Ge at 800°C is in good agreement with reported values.[18]

An obvious result of the above experiment is that the As diffusion into the p-Ge is much too deep for our device using the 800°C diffusion temperature and the usual MC-VPE GaAs growth temperature of 750°C. Therefore, a second series of MC-VPE GaAs/Ge samples was grown in which there was no prior As diffusion before GaAs growth. The only variable which was changed was the GaAs growth time. A constant 750°C growth temperature was used. Fig. 11 summarizes the results of this series. The As diffusion

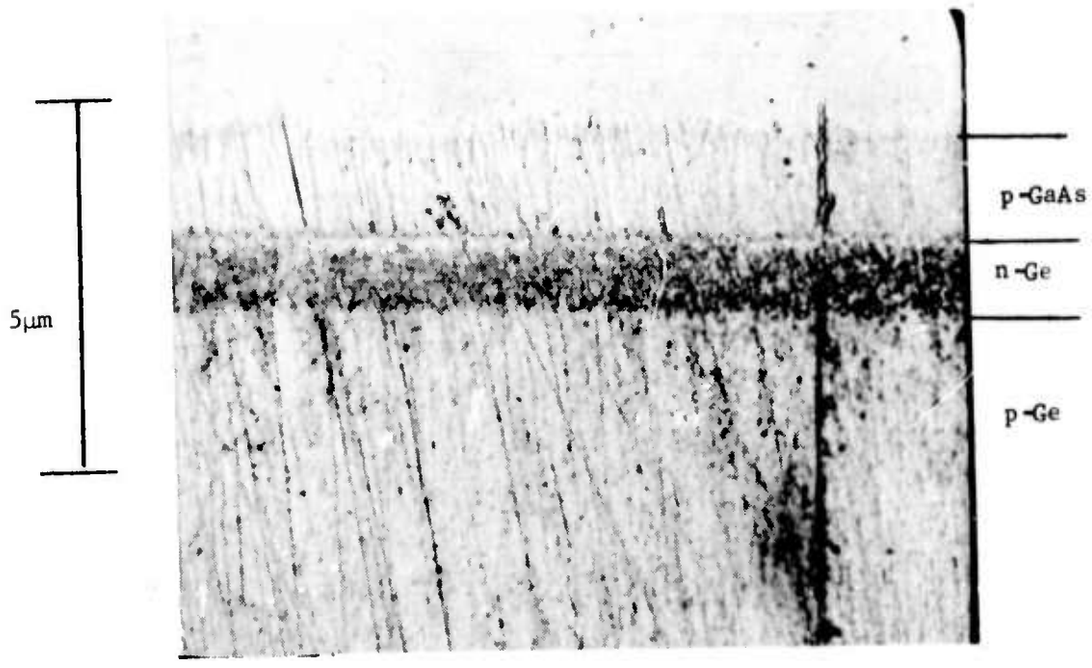

Fig. 9. 5^{o} angle lap with Cu n-stain on sample #9-12-72:1. This was a 2-minute GaAs growth at 750^{o}C and Zn doped.

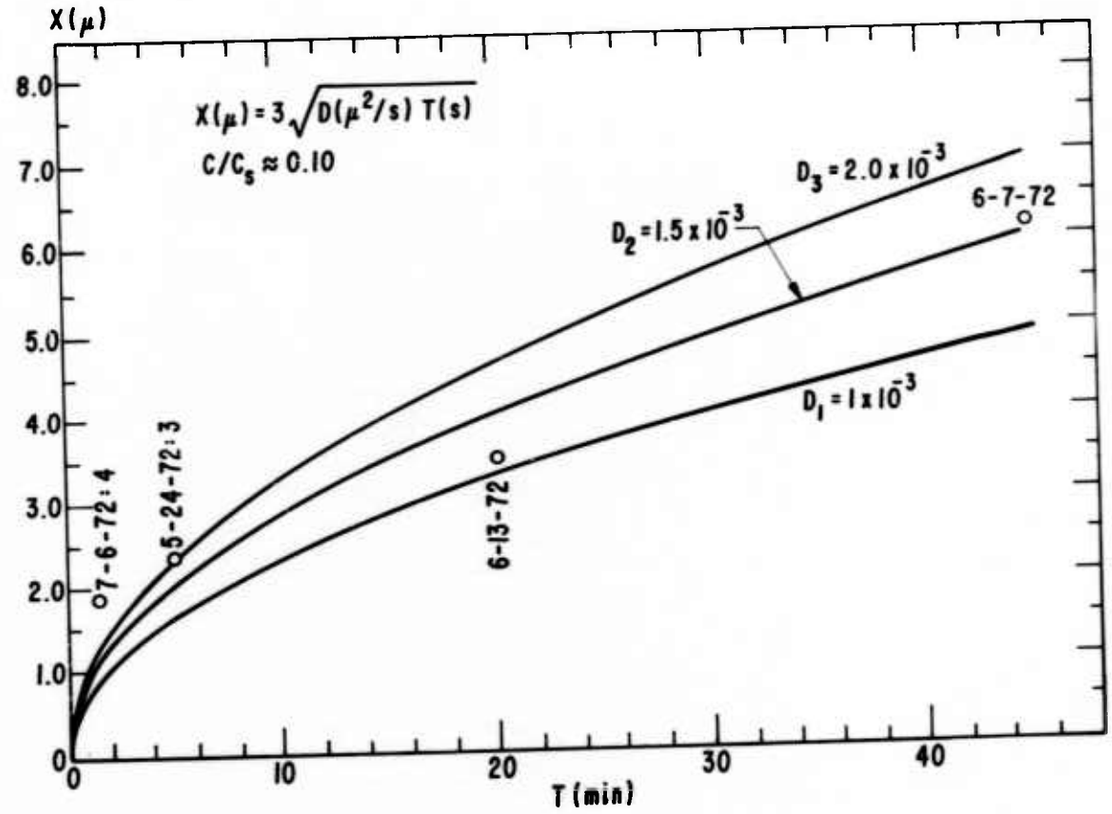

Fig. 10. Depth of As diffusion into p-Ge versus time of diffusion at 800°C. The four data points are shown as circles on this plot. The three curves are theoretical diffusion depth curves for three different diffusion coefficients, D = 1.5±0.5x10-3 microns^2/sec. The "constant surface concentration" boundary condition was assumed in these calculations and the boundary of the p-n junction was assumed to be seen in the angle lap photographs when the boundary concentration to surface concentration ratio C/C_s was taken to be approximately 0.10.

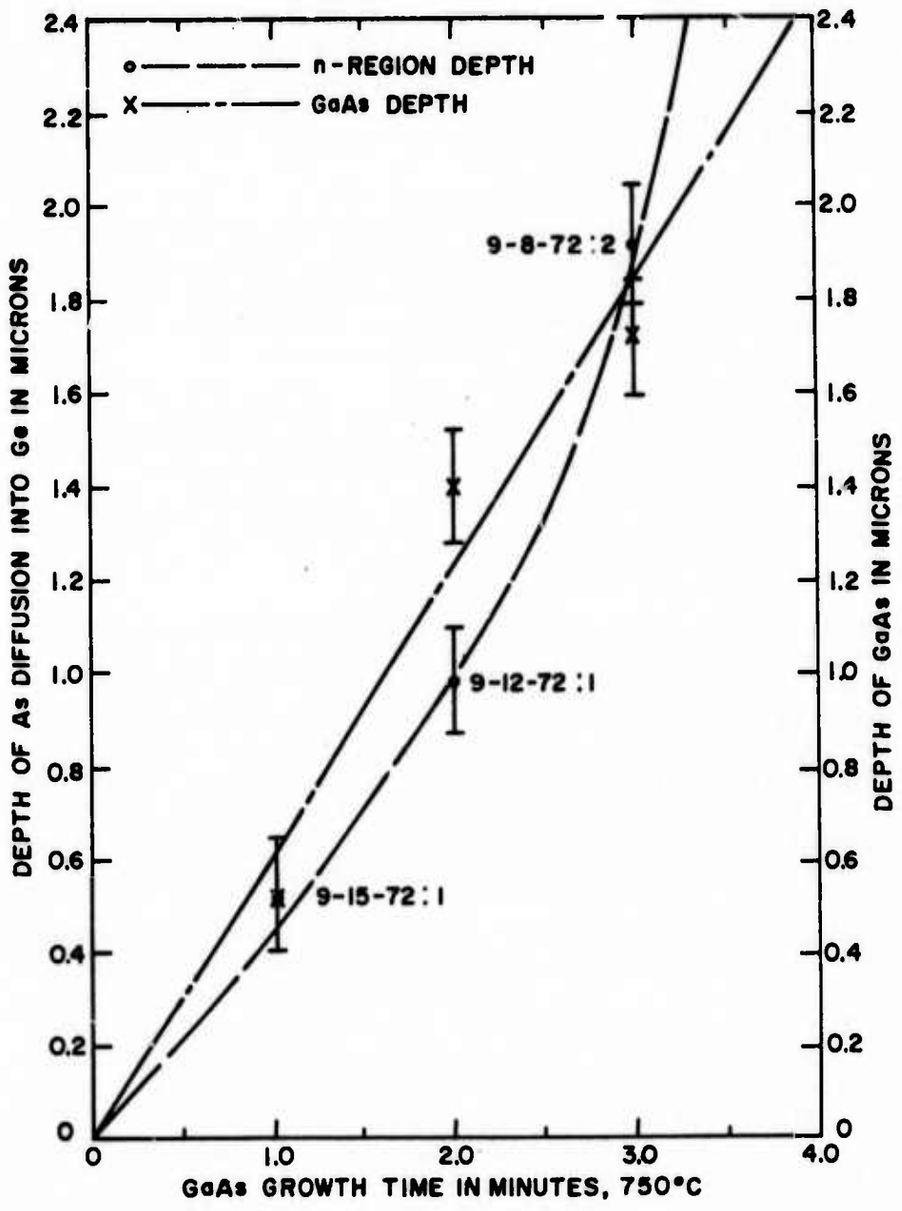

Fig. 11. Depth of As diffusion into the p-Ge wafer and thickness of the epitaxial GaAs vs growth time in minutes at 750°C.

depths are much smaller - but still, at best, a factor of approximately 10 too great. Also note that the thickness of the GaAs and the depth of the As diffusion are roughly equal. As a result, it would appear that achieving a 0.1 to 0.2 micron thick GaAs layer with a 250-500 Å deep As diffusion is impossible with the MC-VPE growth system using 750°C as the growth temperature.

The only other convenient variable at hand is the growth temperature. The effect of temperature on the As diffusion is very strong as seen in Eq. (8). A third series of MC-VPE GaAs/Ge samples was grown with no prior As diffusion; a constant growth time, 90 seconds; and varying the growth temperature from 750°C to 600°C. Fig. 12 summarizes the results of this experiment. The experimental points were measured from angle lap and staining photos, and the linear behavior is consistent with Eq. (11). We note at once that the required thin diffusions are possible by going to growth temperatures of approximately 600°C. Visual examination, however, of samples grown at 625 and 600°C show largely polycrystalline growth. Figs. 13, 14, and 15 show the deterioration of the epitaxial growth with reduced growth temperature. Note that these samples are not Zn doped.

The poor quality GaAs films grown at the reduced growth temperatures coupled with the Ge autodoping problem noted in Section E led us to completely abandon the MC-VPE process for our device. The remainder of the contract has focused on GaAs/Ge grown by the organometallic vapor-phase technique. This is a promising growth method for our device for two reasons. First, the growth temperatures are 100 to 150°C lower than for MC-VPE and, second, there are no active by-products of the growth process. The quality of the GaAs/Ge grown by OM-VPE is excellent as seen by the good activation levels achieved and discussed in Section F.

Table II summarizes the results of a number of OM-VPE GaAs/Ge growths made under different conditions. Two things are apparent from these results. First, the typical n-Ge As diffusion depths are smaller by a factor of 2 to 10 than those of samples grown by MC-VPE. This is most likely due to the 100-150°C lower growth temperature. Second, the depth of As diffusion for all but sample #935 is still too deep. The main reason for this is that all samples but #935 were intentionally exposed to arsine prior to GaAs growth. Also, many of them were grown at 660°C instead of at 630°C. The higher growth temperature generally gives a deeper As diffusion which is consistent with our experience with MC-VPE GaAs/Ge samples. (630°C is approximately the lowest practical GaAs growth temperature consistent with good quality GaAs growth on Ge using the OM-VPE process.) Sample #935 is particularly significant in that the GaAs is approximately the right thickness, according to our calculations, while the n-Ge region is extremely narrow - less than 1000 Å, i.e., below the thickness resolution of our angle lap and staining procedure. Note in Table II, that, for the samples marked with a double asterisk (**), the n-stain most likely did not work effectively since the depth of the n-Ge region for these

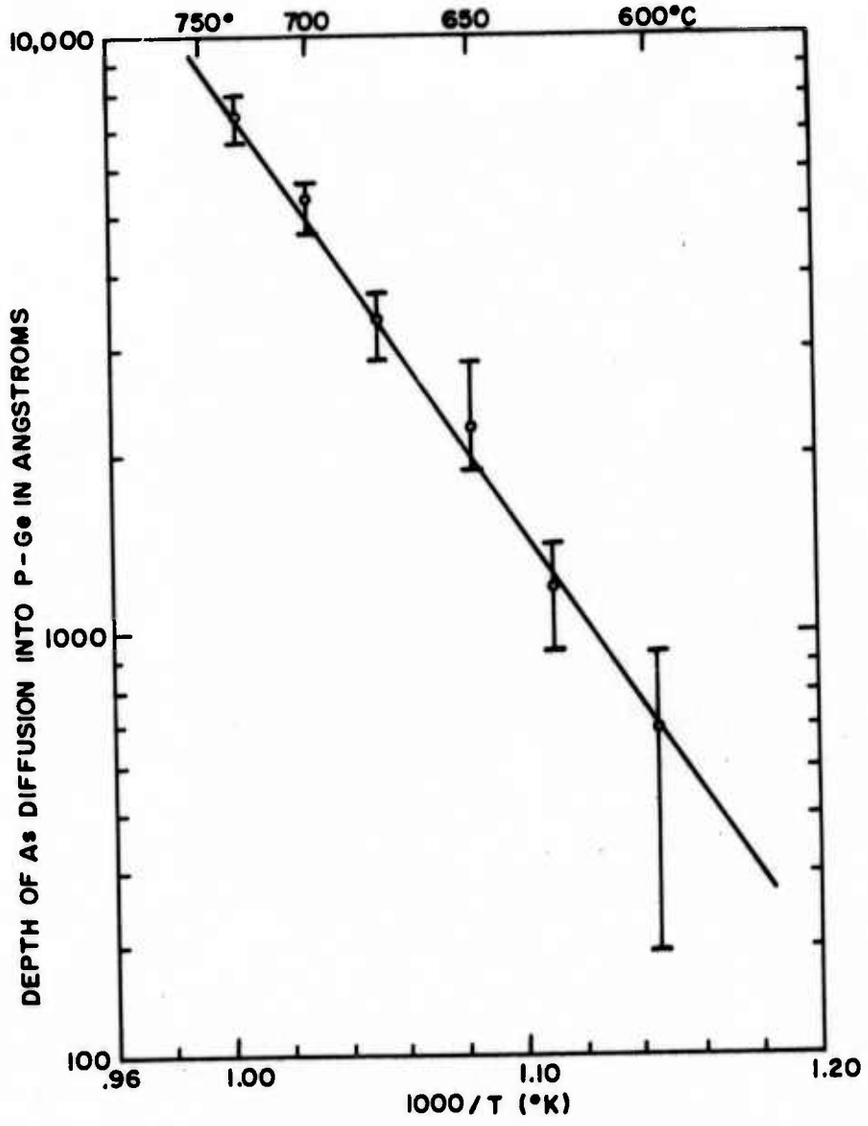

Fig. 12. Depth of As diffusion into p-Ge wafer material vs 1000/T(^{o}K) for constant growth time of 90 seconds. T is growth temperature in ^{o}K. The GaAs thickness for this data varied from 0.7 μm to 0.9 μm - much thicker than the optimal GaAs thickness of ~0.1 μm based on recent calculations (see Appendix).

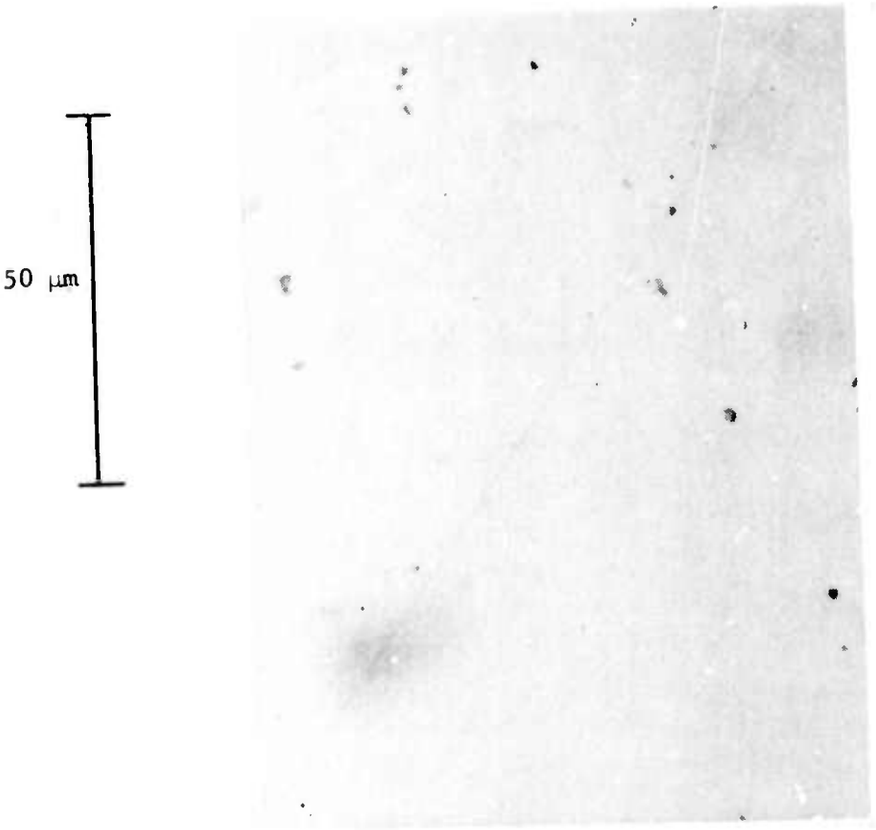

Fig. 13. 650°C GaAs on Ge growth for 1.5 minutes, sample #10-25-72:2, no Zn doping. This sample looks bright and shiny to the unaided eye.

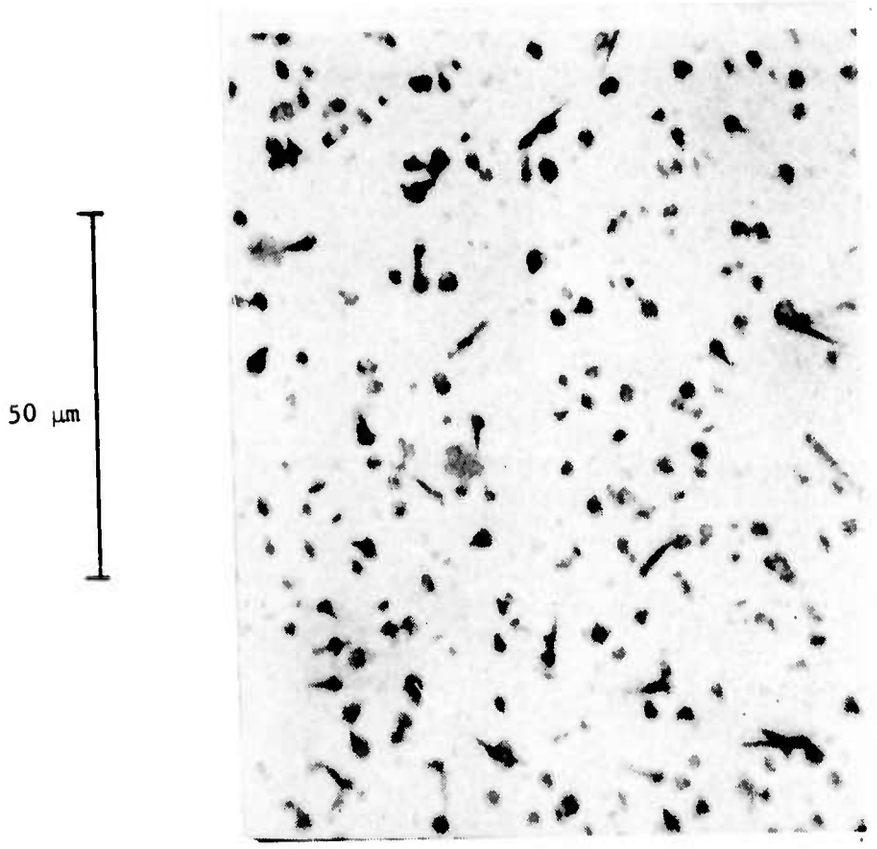

Fig. 14. 625°C GaAs on Ge growth for 1.5 minutes, no Zn doping, sample #10-25-72:1. This sample looks hazy to the unaided eye.

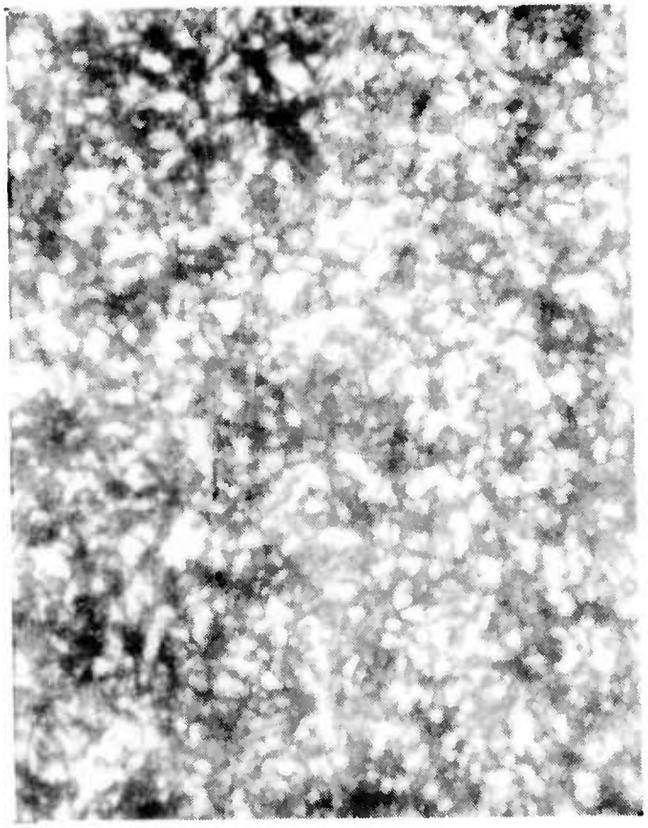

500X

Fig. 15. 600°C GaAs on Ge growth for 1.5 minutes, no Zn doping, sample #10-23-72:2. This sample looks like dull polycrystalline growth to the unaided eye.

Table II

Summary of 5° Angle Lap on GaAs/Ge OM-VPE

Sample Number	Substrate Number	Substrate Polish	Growth Temperature (°C)	Growth Time (min)	GaAs* (μm)	n-Ge* (μm)	As Time
689	62173C	In	630	2	1.6	.4	1 min
728A	LC925	In	660	3	1.6	.9	1 min
729A	LC925	In	600	1.5	.7	<.1**	1 min
730A	LC925	In	630	1.5	.7	∿.1**	1 min
731A	LC925	In	660	1.5	.9	∿.1**	1 min
811	5.5 Ω-cm	Out	660	2	.55	.7	15 sec
812	5.5 Ω-cm	Out	660	2	1.0	.5	30 sec
813	5.5 Ω-cm	Out	660	2	.85	.5	45 sec
814	5.5 Ω-cm	Out	660	2	.85	.5	30 sec
818A	5.5 Ω-cm	Out	660	2	.8	.4	30 sec
818B	LC925	In	660	2	.7	.2	30 sec
821A	LC925	In	660	2	.8	.35	45 sec
822A	LC925	In	660	2	.8	<.1**	30 sec
823A	LC925	In	660	2	.8	.2	30 PH_3 15 AsH_3
857A	LC925	In	660	1	.5	.5	30 sec
857B	LC925	In	660	1	.5	.4	30 sec
914A	LC925	In	660	1/2	.2	.5	30 sec
915A	LC925	In	660	3/4	.3	.6	30 sec
935	5.5 Ω-cm	In	630	1/2	.3	≤.1	0

*Measured from 5° angle lap and staining technique.

**n-stain probably failed on these angle laps.

samples is anomolously low. The angle lap and staining procedure, however, was repeated three times on different parts of sample #935 to confirm that the n-Ge depth was indeed less than 1000 Å. We believe that sample #935 represents a material whose properties are so close to ideal that serious vacuum photoemission testing seemed justified. All attempts to vacuum test this and other samples have been frustrated by premature diode breakdown due to diode heating in vacuum. Details of these experiments are disucssed in Section H.

The maximum solubility of As in germanium at approximately 800°C is $2x10^{20}/cm^3$.[19] As a rough measure of the concentration of As diffusing into our germanium, a lightly doped, 5.5 ohm-cm, Ge substrate was exposed to arsine at 800°C for 45 minutes. The resistivity of the n-type skin was measured using a standard four point probe technique.[20] The thickness of the diffused layer, 12.0 microns, was measured by angle lap and staining procedures. The resistivity was then computed to be $1.2x10^{-3}$ ohm-cm which corresponds to an n-type concentration of approximately $3x10^{19}/cm^3$.[21] The experiment was repeated once again, but this time phosphine was used as the dopant gas. A lightly doped wafer was exposed for 45 minutes at 770°C. The depth of diffusion was much smaller, approximately 1.5 microns. However, the resistivity was measured to be $2.2x10^{-3}$ ohm-cm, corresponding to an n-type doping concentration of approximately $1x10^{19}/cm^3$. Therefore, both As and P enter the Ge in about the same concentration, but the diffusion rates are very different. Very thin (less than 1000 Å) diffused junctions are easily possible with P diffusion into Ge. This result suggests the possibility of using InP/Ge instead of GaAs/Ge. InP does have a lower band gap by about 0.1 eV and does achieve NEA. However, the lattice mismatch between InP and Ge is rather bad, 3.8%. This would most likely lead to a very high density of interface states which may yield severe recombination centers for minority carrier electrons. Nevertheless, there are enough interesting features of InP to justify trying it if the GaAs/Ge device shows some feasibility.

There are two major electrical requirements that the Ge p-n junction must satisfy for optimal device performance. First, the breakdown voltage and reverse saturation current should be reasonably close to the best values reported for Ge, $\leq 10^{-4}$ amps/cm^2. Second, the p-n junction must be able to survive the heat cleaning cycle used in the Cs-O activation procedure of the GaAs. We have not been able to solve the second requirement in the time period of this contract. Initial attempts to observe diode I-V characteristics were frustrated in two ways. First, areas larger than about 5 mm by 5 mm had shorted junctions, probably due to inclusions of localized defects within the area causing breakdown. Second, steel probes were used initially whose pressure on the GaAs surface tended to cause permanent breakdown of a previously good junction.

These initial problems were solved by first evaporating approximately 1 mm diameter, 1000 Å thick gold ohmic contacts onto the top GaAs surface.

Then, small pieces of Hard Wax W were melted over the gold ohmic contacts. The wax was allowed to melt into roughly circular areas of 1-5 mm diameter. Four to six such areas separated by GaAs can be formed onto a single wafer. The wafer was then etched in a 97% HNO_3,3% HF solution at room temperature for 30 minutes. The etch was successful in etching back about 20 microns of the exposed wafer. The Hard Wax W was then washed away in TCE. The resulting mesa structure consisted of islands of GaAs/Ge(n)/Ge(p) separated by p-Ge substrate material. The mesa diodes were initially tested for I-V characteristics using a Tektronix Type 575 curve tracer using a steel probe into the p-Ge substrate material and a 10-mil gold wire probe with a rounded end onto the ohmic gold GaAs contact. Good IV characteristics were observed on about 50% of all mesa diodes tested in this way. Figs. 16 and 17 are I-V curves of typical diffused Ge junctions for 0.02 and 5.5 ohm-cm p-Ge substrate material, respectively. The 0.02 and the 5.5 ohm-cm resistivities correspond to approximately $4x10^{17}$ and $6x10^{14}/cm^3$ acceptor doping concentration, respectively.[21] The diffused n-Ge is approximately $10^{19}/cm^3$ as mentioned above. Assuming our diffused junctions are one-sided abrupt junctions, we can use Sze and Gibbons' results[22] to judge the extent to which our reverse breakdown voltages in Ge approach the "ideal". The reverse breakdown of the more heavily doped p-Ge junction is about 2.0 volts and is reasonably close to the ideal reverse breakdown voltage. The 60.0 volt reverse breakdown voltage for the lighter doped p-Ge junction is about a factor of two to three down from Sze and Gibbons' data. The reason for this discrepancy is not clear. However, there are several possible explanations. First, when one of our diodes does breakdown, the breakdown occurs most often at the edge of the mesa. Therefore, it is possible that the 60.0 volts is not a true bulk breakdown but, rather, edge breakdown. Second, the saturation current from our mesa type diodes is often rather high. This fact also suggests a surface leakage problem but could also result from excessive bulk damage in the Ge junction region due, perhaps, to a poor polishing job on the Ge or to poor quality germanium. Section H discusses this problem in more detail.

H. Device Fabrication and Testing

In this section, we describe some of the more significant fabrication and testing methods we have employed during the course of this contract. Diode fabrication, photovoltaic and electroluminescence measurements, and vacuum diode testing are discussed below. The vacuum activation of GaAs/Ge was discussed in some detail in Section F.

1. Diode Fabrication

Most of our experimental studies on diodes have been on mesa-type devices. The fabrication of these diodes is discussed in Section G. The mesa-type diode fabrication procedure has been successful in making reasonably low leakage diodes ($\lesssim 10^{-4}$ amps/cm^2 at -1.5 volts) as large as 5 mm by 5 mm from GaAs/Ge wafers. However, this is the exception; most diodes larger than approximately

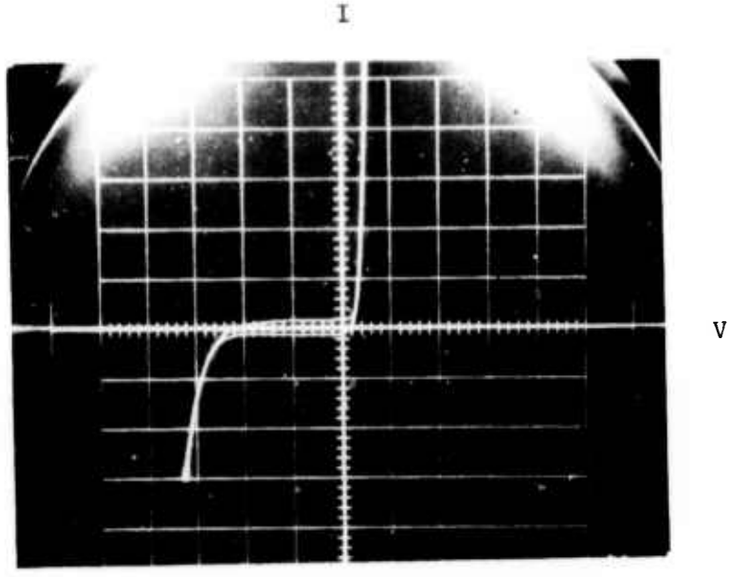

50 μA/div vertical
0.5 V/div horizontal

Fig. 16. Ge p-n junction I-V characteristic for the ≈.02 ohm-cm p-Ge Ga-doped wafer material. Substrate #LC925, MC-VPE sample #9-8-72:1. Note that this particular sample was given a normal heat cleaning cycle used for our Cs-O activation procedure of the GaAs. The mesa diode and I-V characteristic were both made after this heating. This is a typical I-V for this material. Typical diode areas are .03-.80 cm^2.

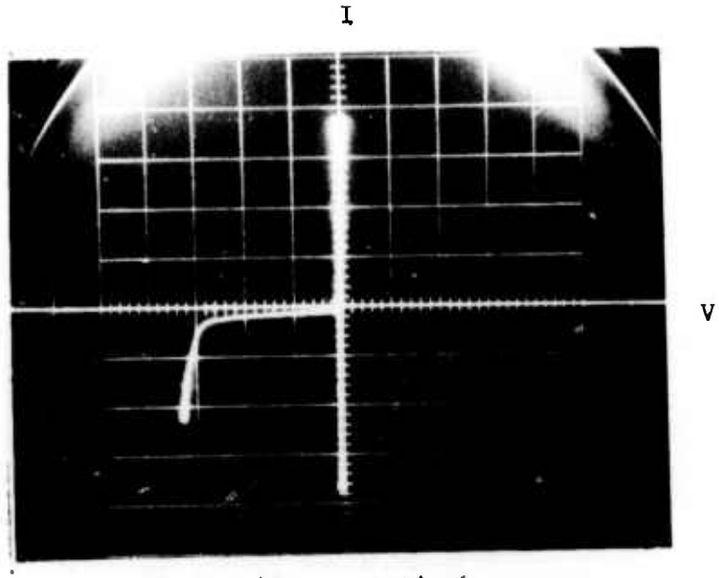

1.0 mA/div vertical
20. V/div horizontal

Fig. 17. Ge p-n junction I-V characteristic for the 5-6 ohm-cm p-Ge Ga-doped wafer material. Substrate #Ge62173C, MC-VPE sample #10-3-72:2. Note the much higher reverse breakdown voltage in comparison with the .02 ohm-cm Ge material, as expected. Diode area is approximately 0.12 cm^2.

3 mm in diameter suffer from high leakage. The source of this leakage is thought to be associated with edge breakdown since slightly smaller low leakage diodes can very often be fabricated from previously poor mesa diodes. Also, in general, our experience has been that the smaller the edge perimeter of the diode, the more likely that the diode will have low leakage. All photovoltaic and electroluminescence measurements have been made on mesa-type diodes.

In addition to mesa-type diodes, we have, during the last few months of this contract, been working on the fabrication of planar-type diodes on Ge wafers. The planar-type diode is thought to be more resistant to premature edge breakdown - especially upon diode heating in vacuum. The mesa-type diode is not a passivated diode. The p-n junction edge is exposed at the perimeter of the etched mesa. A planar-type diode has a passivation layer which serves to delineate the size and shape of the junction but also covers the junction edge. Our original attempts to make a planar diode were based on e-beam evaporated SiO_2, approximately 1500 Å thick. After a p-Ge wafer was coated with SiO_2, it was then masked with black wax to delineate a number of different sized areas ranging from 1x1 to 4x4 mm. After the black wax had dried (about 12 hours at 50°C), the exposed holes in the black wax mask were etched with $1HF:2H_2O$ for 5 minutes at 25°C. This HF etch removes the SiO_2 but does not significantly etch the Ge wafer. The black wax mask is then removed with TCE leaving an SiO_2 on Ge mask with holes. In order to fabricate p-n junctions, we then exposed these prepared wafers to arsine or phosphine for 5 to 15 minutes at approximately 775°C. The As and P are the n-type dopants which will rapidly diffuse into the exposed Ge in the SiO_2 mask but, ideally, should diffuse very slowly into the polycrystalline SiO_2. Diodes formed in the above manner using the e-beam evaporated SiO_2 were ohmic in every case. The reason for the failure of these diodes is thought to be twofold. The quality of the SiO_2 formed on Ge using the e-beam technique is not regarded as being very good;[23] pin holes or cracks in the film can easily be sources of diode failure. Also, the thickness of the SiO_2 film probably is not sufficient to prevent diffusion of the arsine or phosphine through the film and into the Ge. For these reasons, we have been using most recently SiO_2 grown on Ge by the silane process.[24] This is the process that is sometimes used commercially for MOS devices. Relatively thick layers can be grown by this process (up to 1.0 micron), and the film quality is generally very good. Our only experiments to date using SiO_2 films grown in this fashion have been on films approximately 6000 Å thick as calculated from counting interference fringes formed by monochromatic light. Holes were masked and etched into the film as before. Again, the masked SiO_2:Ge wafers were exposed to phosphine to form junctions. Good junctions were formed this time with 5 minute phosphine exposures. Fig. 18 shows a typical I-V characteristic from such a planar passivated Ge diode. Wafers that were exposed for 15 minutes, however, showed consistently ohmic diodes. The failure of these diodes is thought to be due to phosphorus diffusion through the passivation film. This conclusion is tentative and needs to

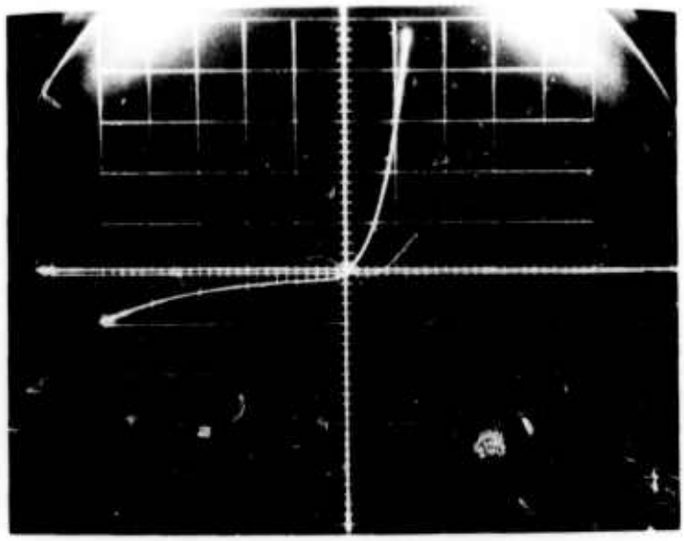

50 μA/div vertical
0.5 V/div horizontal

Fig. 18. Ge p-n junction I-V characteristic for .02 ohm-cm p-Ge Ga-doped wafer material. This diode is a planar-type diode fabricated using approximately 6000 Å thick silane-grown SiO_2 as a passivation layer. This diode does not have GaAs grown on the p-Ge but, rather, the wafer was exposed for 5 minutes to phosphine at 775°C. The junction depth is only 0.2 to 0.3 micron. The diode area is $\sim$0.2 cm^2.

be investigated in more detail. One important variable that needs to be examined is the degree to which the SiO_2 film is densified prior to exposure to phosphine. For the case of our diodes, the SiO_2:Ge wafers are preheated in a hydrogen atmosphere until the wafer achieves the desired diffusion temperature, 775°C. The preheat cycle of approximately 5 to 10 minutes should be sufficient to densify SiO_2. It is possible, however, that the films are not sufficiently densified prior to phosphine exposure in which case the atomic diffusion of phosphorus into the SiO_2 would proceed much more rapidly. No photovoltaic or electroluminescence measurements have been made on planar-type diodes. However, vacuum diode testing has been initiated, and results are available on two different wafers of planar-type diodes.

2. Photovoltaic Measurements

Based in part on our activation results summarized in Table I, we have constructed a probable energy band diagram for MC-VPE and OM-VPE grown GaAs/Ge as shown in Fig. 19 (A) and (B). The MC-VPE grown GaAs/Ge, we believe, has a rather thick, ∿0.3 μm, initial growth region of n-type GaAs before p-type growth begins. We have made a series of photovoltaic measurements on thick and thin GaAs/Ge samples grown by both MC-VPE and OM-VPE. The most interesting results, however, are seen on the thick, ∿5 micron, GaAs/Ge samples. Fig. 20 shows photovoltaic response (relative) versus incident light wavelength for a thick GaAs/Ge MC-VPE sample. The measurements were made using a Cary 14 spectrophotometer modified to automatically plot relative quantum response versus wavelength. Mesa-type diodes, masked by black wax to expose only the active part of the mesa diode to the incident light, were used for these experiemtns. The photovoltaic response from approximately 0.8 to 1.9 microns in Fig. 20 is believed to be due to the Ge p-n junction. It is likely that photoexcited electrons in the bulk p-Ge wafer are being collected by the Ge junction and are responsible for most of this signal. A few photoexcited holes are generated in the n-Ge region. However, their contribution to the total signal is probably small since the thickness of the n-Ge is on the order of only a micron. The photovoltaic response from 0.4 to 0.7 micron, however, cannot be associated with the Ge. Light of these wavelengths is strongly absorbed in the GaAs. Note that this signal is a factor of ten lower but also is of the opposite polarity. These facts suggest strongly that this signal is from photoexcited holes in the n-GaAs region which then diffuse into the p-GaAs region and are collected. Photoexcited electrons in the p-GaAs region which diffuse into the n-GaAs region would also produce a signal of this polarity. However, the p-GaAs is quite thick, as much as 5 microns. Hence, photoexcited carriers generated in the p-GaAs would most likely recombine before diffusing far enough to be collected in the n-GaAs region. For this reason, we feel that the photovoltaic response seen from 0.4 to 0.7 micron is strong support of the energy band diagram outlined in Fig. 19A for MC-VPE GaAs/Ge.

Figure 21 shows the measured photovoltaic response from a thick GaAs/Ge sample grown by OM-VPE. The response from 0.9 to 1.9 microns is

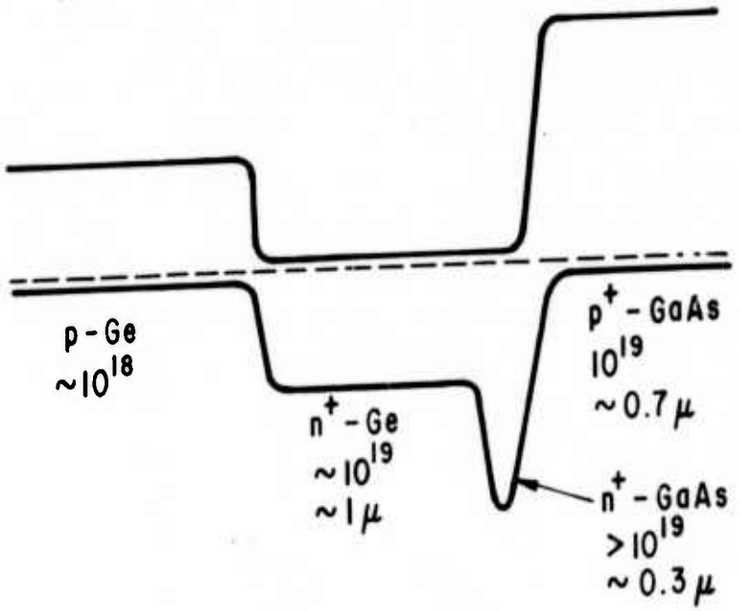

GaAs/Ge, MC-VPE
(A)

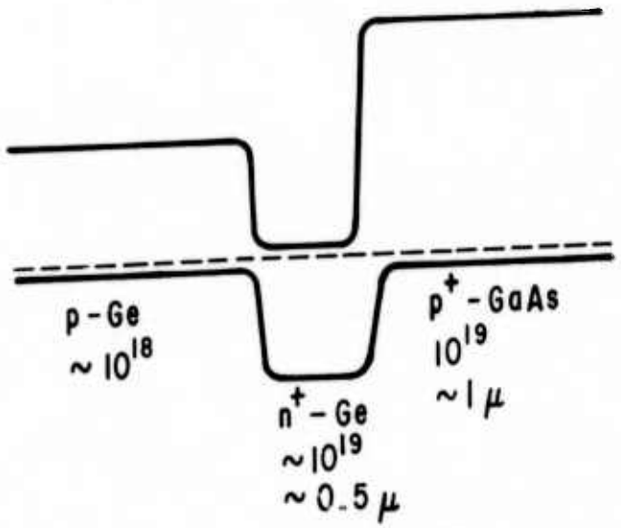

GaAs/Ge, OM-VPE
(B)

Fig. 19. Derived energy band diagrams for MC-VPE GaAs/Ge (A) and OM-VPE GaAs/Ge (B). These diagrams are consistent with photoemission and photovoltaic measurements.

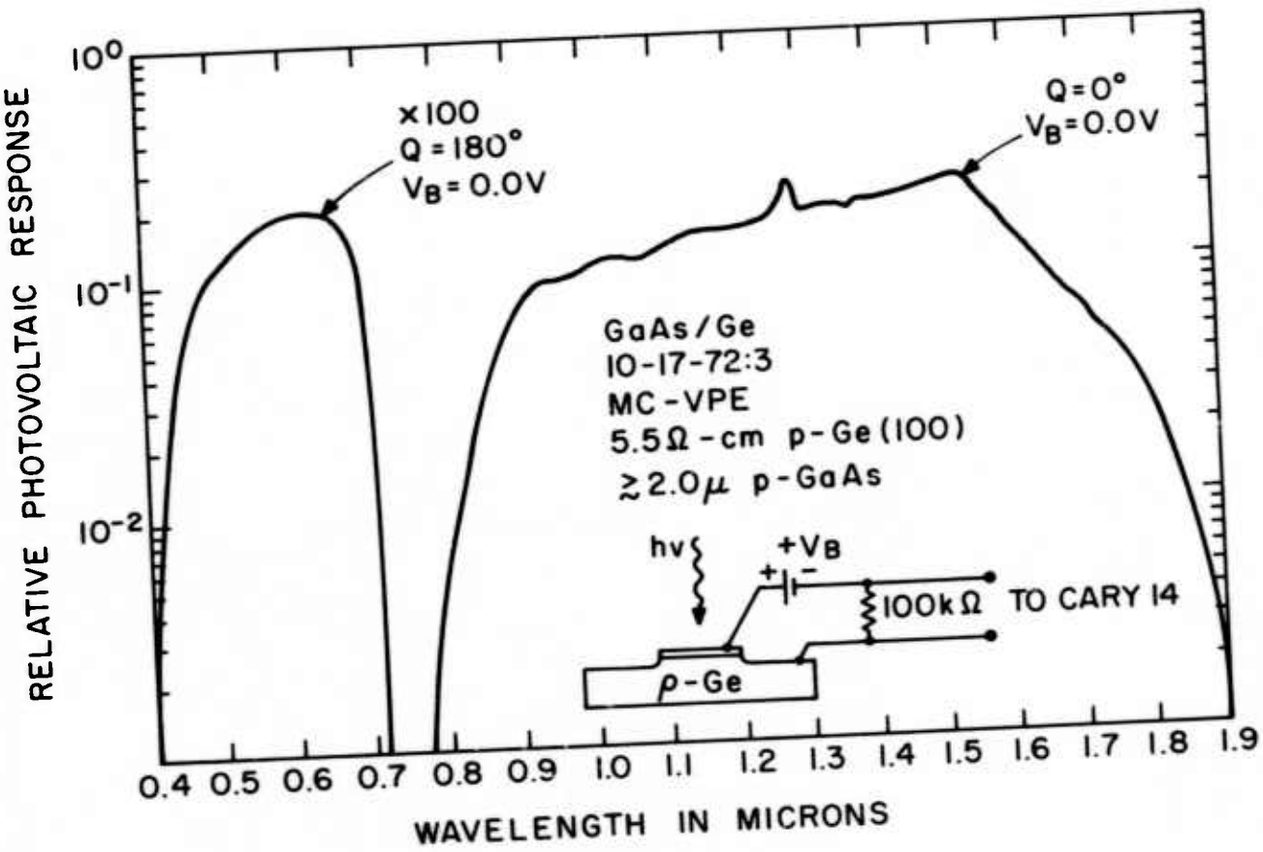

Fig. 20. Relative photovoltaic response versus wavelength curve from a MC-VPE GaAs/Ge sample. The GaAs is relatively thick, ≳2.0 μm. Note that the 0.4 to 0.7 μm response is ∿X100 down in signal strength from the 0.8 to 1.9 μm signal.

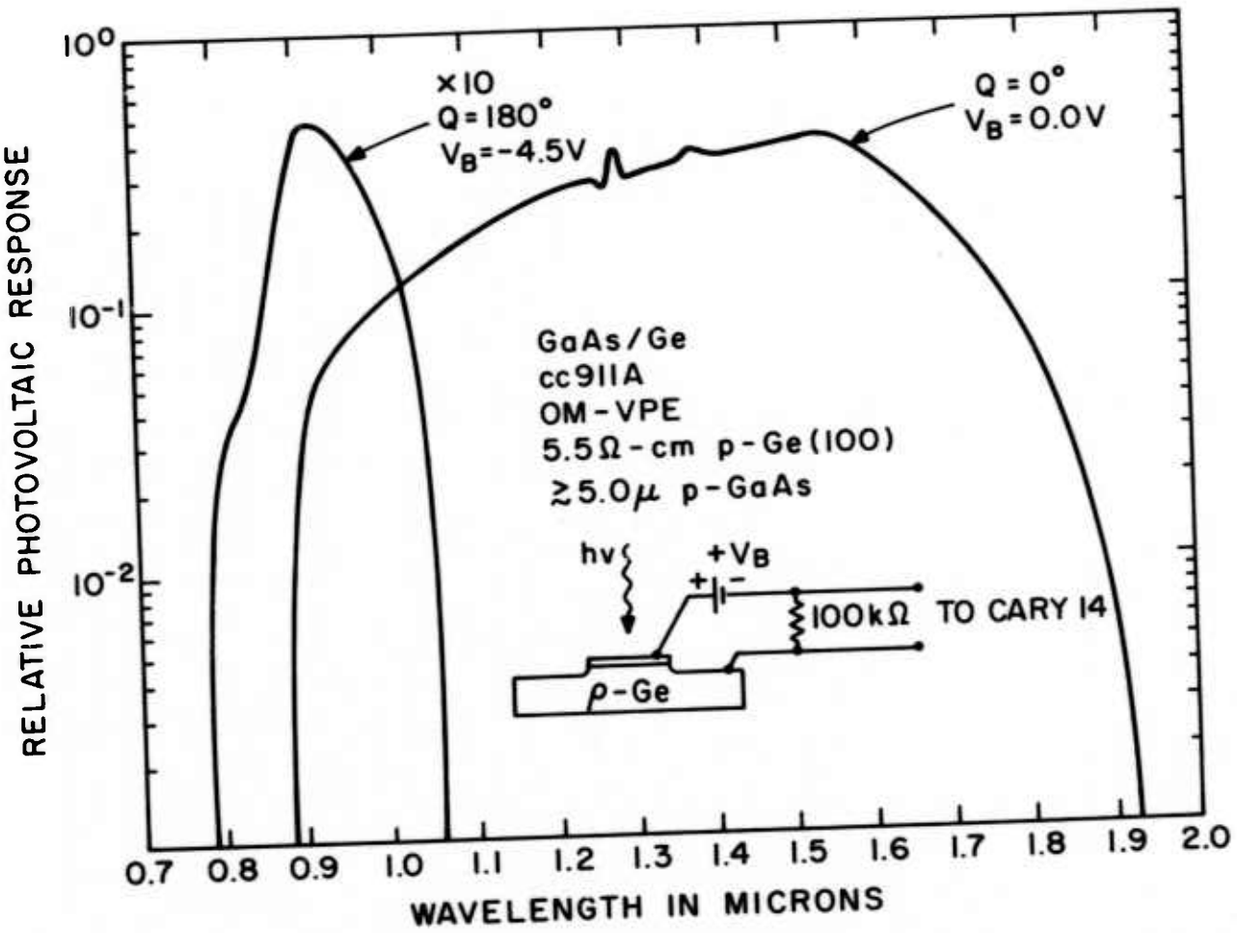

Fig. 21. Relative photovoltaic response versus wavelength curve from an OM-VPE GaAs/Ge sample. The GaAs is relatively thick, ≳5.0 μm. Note that the 0.8 to 1.05 μm response is ∿X10 down in signal strength from the 0.9 to 1.9 μm signal. A -4.5 V bias voltage was needed to see the 0.8 to 1.05 μm signal.

most likely from the Ge p-n junction. The sign of this response is consistent with photoexcited electrons in the p-Ge wafer diffusing into the n-Ge and being collected. Note that in this figure and Fig. 20 there is a ripple in the curve around 1.27 microns. This ripple is a well known spurious effect associated with the Cary 14 and is not a true photovoltaic response behavior.[25] The photovoltaic response from 0.8 to 1.15 microns in Fig. 21 is quite different than that seen for the MC-VPE GaAs/Ge sample. First, note that this signal is seen only in the presence of a negative bias voltage. Also note that the sign of the signal is opposite to that of the Ge p-n junction signal. Furthermore, the peak of this response is near 0.9 micron. GaAs is nearly transparent at 0.9 micron. Hence, the measured response from 0.8 to 1.15 microns is probably not due to GaAs but to photoexcited holes in the n-Ge which diffuse into the p-GaAs and are collected. Since we see no zero bias photoresponse from 0.4 to 0.8 micron analogous to the GaAs p-n junction response of Fig. 20, we conclude that there is probably no n-GaAs present. Therefore, GaAs/Ge grown by OM-VPE results in a true heterojunction which is essential for the successful operation of this device. Again, the measured photovoltaic response from the OM-VPE GaAs/Ge sample is consistent with the energy band diagram outline in Fig. 19B. Overall, then, the photovoltaic response measurements are consistent with the proposed energy band diagrams of Figure 19 but are not conclusive proof for their validity.

We have made additional photovoltaic response measurements on thin ($\lesssim$1.0 micron) GaAs/Ge samples grown both by MC-VPE and OM-VPE. In general, these measurements do not yield as much information as those of Figs. 20 and 21. For zero bias, thin GaAs/Ge photovoltaic response curves show a Ge p-n junction behavior from approximately 0.5 to 1.9 micron. The onset of photoresponse, 0.4 versus 0.5 micron, for example, depends only on the thickness of the GaAs. We have looked for additional GaAs-related photoresponse using different magnitude and polarity of bias. However, the strength of the Ge p-n junction signal is so great as to swamp any weak photoresponse from the thin GaAs. The thin GaAs/Ge grown by MC-VPE did show a very weak GaAs p-n junction response under -6.0 volt bias; however, the signal was more than 10^3 down from the peak Ge p-n junction response. Finally, we note that the Ge p-n junction response itself does respond to an applied bias. Reverse biasing this junction enhances the signal as much as a hundred-fold, depending on the strength of the bias while forward biasing the Ge p-n junction reduces the Ge photoresponse. The effect of an applied bias on the Ge photoresponse is much larger on the lightly doped ($\sim 10^{15}/cm^3$) p-Ge substrate material than on the more heavily doped material ($\sim 10^{17}/cm^3$). This observation is consistent with the fact that the effective junction depletion layer width under bias is much wider for lighter doped p-Ge.

3. Electroluminescence Measurements

We have been successful in observing GaAs electroluminescence from an OM-VPE GaAs/Ge sample. The GaAs was approximately 1.0 micron thick, and

the wafer was divided into three mesa diodes. Each mesa was outlined with black wax so that only the GaAs is uncovered. The edges of the mesa are covered. The wafer was placed under a microscope outfitted with an S-1 image intensifier and therefore capable of seeing GaAs electroluminescence. Each mesa was then reverse biased (relative to the Ge p-n junction) and light output was sought. Two mesas failed to show any output. However, the third did show definite light output. The diode had to be biased until 50 to 100 mA reverse current was being drawn, on a pulsed basis. Our interpretation is that the Ge diode is in a heavy avalanching mode; a fraction of these hot electrons from the Ge diode are successfully entering the GaAs, thermalizing, and radiatively recombining in the GaAs. Similar measurements were made on MC-VPE grown GaAs/Ge mesa diodes. No electroluminescence was detected from these diodes.

The observation of electroluminescence from our device is quite significant. It means that it is possible to transport hot electrons from Ge into the GaAs emitting layer. The electroluminescent measurement described above was not a quantitative measurement, and, hence, the relative efficiency of electron transport could not be estimated. Additional electroluminescence measurements should be made, however, to study the uniformity of emission and to obtain some estimate of the relative output.

4. Vacuum Diode Testing

The final testing phase of our device consisted of placing a wafer of isolated GaAs/Ge diodes into our all-metal ultrahigh vacuum system in order to test each for field assisted photoemission. A necessary requirement for the optimum operation from our device is the achievement of NEA on the GaAs surface. At present, the only known way to achieve NEA on a semiconductor surface is to use a sputtering and heating procedure or a heating only procedure in order to obtain a suitably clean surface. In the case of GaAs, the heating procedure is typically from 10 to 60 seconds of heating at 500 to 600°C. It is essential, therefore, that the device diodes be able to withstand a heating cycle of this kind. Our experience to date, however, has been that both mesa and planar-type diodes become ohmic for typically 10 to 20 seconds heating at 400°C or higher. This experimental fact has been responsible for the lack of vacuum photoemission experiments during the course of this contract.

Almost all our vacuum diode testing experience has been with mesa-type diodes. We have found that approximately half the mesa diodes on a given wafer break down after only baking out the vacuum system (250°C for 16 hours). The remaining good diodes can be exposed to Cs or Cs and O_2 without noticeable changes in the I-V characteristics. However, as mentioned above, a few seconds heating to 300 to 400°C will, without exception, result in ohmic diodes. The ohmic breakdown occurs independent of whether the diodes had been previously exposed to Cs at any time or not. The ohmic diodes can be removed from the vacuum system, however, and

re-etched. The new diodes fabricated from the remaining ohmic mesas are in almost all cases good. This fact indicates strongly that the diode breakdown is an edge rather than a bulk breakdown. For this reason and because it has been noted that several monolayers of Cs on clean vacuum-exposed junctions can cause heavy edge diode leakage,[26] we have carried out an effort to make and test planar-type diodes from Ge substrates.

For our application, planar-type diodes offer three potential advantages over the mesa-type diodes. First, the junction edge being buried under a suitable passivation layer may prevent or significantly reduce atomic As migration at the junction which is probably the cause of the mesa diode breakdown. Second, the junction edge in a planar diode would never be in atomic proximity to the Cs-O used to activate the GaAs. Third, the passivation layer used, such as SiO_2, can be doped lightly in such a way as to form a guard ring type structure which could significantly reduce edge leakage problems. Toward the end of this contract, we were successful in the fabrication of planar-type diodes from p-Ge wafers, as previously discussed in Section H-1. Our experiments on vacuum testing the planar-type diodes were limited to only two wafers of diodes prepared in identical fashion. Both wafers had simple phosphorus-diffused planar diodes. There was no attempt to grow GaAs in the exposed Ge holes. The reason for making simple diffused p-n junctions was to avoid the complication that might arise with an extra GaAs layer on top of the diffused Ge p-n junction. The depth of the diffused phosphorus junction was 0.2 to 0.3 micron. Approximately six good junctions were fabricated on each wafer. The wafers were then mounted in the ultrahigh vacuum system. After rechecking the I-V characteristic for good diode behavior after mounting, the system was evacuated and baked out overnight at 250°C. After bake-out, each diode was I-V tested. Approximately half the diodes were ohmic or showed large leakage. The remaining diodes were essentially unchanged from their prebake-out I-V characteristic. One of the wafers was then exposed to Cs and various Cs plus O_2 cycles. The remaining good diodes on this wafer showed no change upon being exposed to Cs and O_2. Field enhanced photoemission was looked for but not observed. However, this fact is not surprising since the junction depth was deliberately too great for hot electron emission, and, furthermore, the n-Ge surface was certainly dirty. Next, the wafer was heated slowly to approximately 400°C for 15 seconds and slowly cooled back to room temperature. This single heat treatment "destroyed" the remaining planar diodes. In every case, the remaining diodes were ohmic. The second wafer of diodes was similarly heat-treated with the same results. The only difference between the two wafers was that one was $10^{18}/cm^3$ p-Ge (100) while the other was $3x10^{17}/cm^3$ p-Ge (100). Overall, the planar-type diode showed no better heat resistance than the mesa-type diodes.

The mechanism of the planar-type diode breakdown, however, may be quite different than the mesa diode breakdown mechanism. There is a possibility that the passivation layer of 6000 Å of SiO_2 is not doing its

job effectively. That is, the passivation layer itself may be shorting out the diodes. During fabrication of the diodes, the n-type dopant, phosphorus in our case, will diffuse into the SiO_2 to some degree. If the P should diffuse completely through the passivation layer, all diodes would test ohmic. We believe we have seen this case when the P diffusion is allowed to continue beyond approximately 10 minutes at 775°C. The good diodes were fabricated using a 5-minute diffusion. It is, therefore, possible that the mild 400°C heating in vacuum drives the diffused P through the remaining SiO_2 and into the Ge below the passivation layer. If this does happen, then all diodes would measure ohmic or at least begin to show large leakage. The cure for this mechanism of breakdown would be to use a thicker passivation layer and/or to dope the passivation layer with a p-type compensating dopant. (Other passivation layers such as Al_2O_3 should also be tried.) These corrective ideas have not tested to date.

In summary, premature diode breakdown in vacuum has been a most difficult problem. Based on a number of different experiemtns using the mesa-type diode, we feel that the mesa diode is not able to withstand even mild conventional heat-cleaning procedures in a vacuum environment. Even if the mesa diode could survive, the application of Cs onto the clean exposed Ge p-n junction may lead to severe leakage. Potentially, the planar-type diode has a better chance for our device. Although the first vacuum experiments on planar diodes were disappointing, there are a number of possible "fixes" that might work. If, after further experiments, it becomes clear that neither the mesa nor the planar-type diode can survive conventional heat-cleaning procedures, then other techniques would have to be investigated. Among these would be the possibility of fabricating the device in the same vacuum system as used to activate and thereby avoiding the necessity of heat cleaning. Another possibility would be to investigate ways of protecting a crystal from the time of growth until placement in the vacuum activation system. These and other possibilities, however, are relatively involved investigations that are more appropriately separate research studies in themselves.

III. CONCLUSIONS AND RECOMMENDATIONS

In this final section, we outline the major accomplishments achieved during the course of this contract and our recommendations for further work in this area.

A. Major Accomplishments

1. Theoretical calculations indicate that a GaAs/Ge or InP/Ge device is capable of 1 to 4% quantum efficiency in transmission at 1.55 μm.

2. Considerations of dark current indicate that cooling will be necessary - perhaps to -80°C.

3. The organometallic vapor phase epitaxy growth method is most suitable for growing the GaAs/Ge device.

4. Ultra-thin diffused junctions (500 Å) can be fabricated using the organometallic process.

5. Thin GaAs (0.3 m) has been activated to NEA with reasonably good escape probability (45%).

6. Photovoltaic measurements show that organometallic grown GaAs/Ge gives ideal heterojunction behavior.

7. Electroluminescence has been observed from the GaAs of a reverse biased GaAs/Ge device.

8. Both mesa and planar-type diodes have been successfully fabricated.

9. Both mesa and planar-type diodes fail to survive moderate heat-cleaning cycles needed to achieve clean surfaces in vacuum.

B. Recommendations for the Future

1. There remains about six months further work to optimize Ge wafer preparation and GaAs growth. Ge polishing and pre-growth preparation is still a problem.

2. A great deal more work is needed on electroluminescence and internal photoemission related experiments to definitely determine the feasibility of the GaAs/Ge hot electron approach to 1-2 micron photoemission. A full year's effort could be spent on non-vacuum, on-the-bench type experiments.

3. A most serious problem faced by our project and others using a biasing approach to enhanced photoemission is that of diode breakdown in vacuum. We have already spent over six months effort trying to solve this problem. At least another six months effort will be needed.

IV. APPENDIX

In this Appendix we discuss in more detail the calculations made for the transmission quantum efficiency of the GaAs/Ge device. In particular, the model and approximations are pointed out. Furthermore, the sensitivities of most of the design variables are shown in the figures which follow.

We begin with a calculation of the transmission quantum efficiency of the flat band p-Ge layer to 1.55 micron radiation. 1.55 micron is chosen since the atmosphere has a window at this wavelength, and germanium is a direct band gap absorber of light at this wavelength. Reference to W. C. Dash and R. Newman, Phys. Rev. 99, 1151 (1955) gives $\alpha \approx 0.5$/micron at 1.55 μm. We shall assume an effective antireflection coating has been applied to the back of the germanium so that the back reflectivity at 1.55 μm is approximately zero. We need to solve

$$-D^2 n(x) + \frac{n(x)}{\tau} = G(\alpha,x) \tag{1}$$

subject to the boundary conditions of

$$D\frac{dn(x)}{dx}\Big|_{back} = Sn(x)\Big|_{back} \tag{2}$$

and

$$n(x)\Big|_{junction} = 0 \quad . \tag{3}$$

The yield in transmission is then given by

$$Y_T = \frac{-D\frac{dn}{dx}}{I_o}\Big|_{junction} \tag{4}$$

where I_o is the incident light intensity, S is the back surface recombination velocity, τ is the electron lifetime, D is the electron diffusion constant, and $G(\alpha,x)$ is the generation function. In general,

$$G(x) = Ae^{+\alpha x} + Be^{-\alpha x} \tag{5}$$

where A and B are functions of the reflectivities of the back and front surfaces, α, and the thickness of the germanium.

We have solved this equation and put its solution onto our time-share computer system. Graphical results for reasonable input values are shown

in Figs. 1A and 2A. Note that, for a wide variety of situations, the optimal germanium thickness is ~3-4 μm. As expected, the back surface recombination velocity S has the largest effect on the transmission yield. It is convenient to express S as a ratio of S/v where $v = L/\tau$, the diffusion velocity. We have taken S/v = 1.0 as a reasonable value. Note, also, that, if thinning the germanium down becomes a problem, even a 10-micron thick layer with L = 10 μm, S/v = 1.0 is 45% efficient. Hence, this part of the GaAs/Ge device is very efficient, and a transmission efficiency of over 50% is most realistic.

We now turn to the p-n junction region and a calculation of the effective efficiency of electron transport across this region. The basic model we use here is that given by R. E. Simon and B. F. Williams, Phys. Rev. Letters 18, 485 (1967) which was based on the work of D. J. Barelink, J. L. Moll, and N. I. Meyer, Phys. Rev. 130, 972 (1963). The Simon and Williams results pertain to the case where ℓ_i, the mean free path for ionization interactions, is much greater than ℓ_p, the mean free path for electron-optical phonon interactions, i.e., $\ell_i/\ell_p \gg 1$. This case is appropriate for the present device. There are two basic solutions to the hot electron transport problem across a junction, one for $E \gg E_o$ and one for $E \ll E_o$ where E is the mean kinetic energy of the electron and E_o is given by

$$E_o = \frac{e^2F^2\ell_p}{3E_p} \quad . \tag{6}$$

In this equation, F is the field in the junction and E_p is the mean energy loss per collision with an optical phonon. Our situation with a germanium p-n junction and ~1-2 volt reverse bias lies between these two cases. Simon and Williams point out that, for such an intermediate case, the two solutions give essentially the same results. Therefore, we have used the $E \gg E_o$ solution which is given by

$$N(T) = \left(\frac{E_g^2}{T^2} - \frac{E_g}{T}\right) \exp\left(-\frac{E_g^2}{4E_oT}\right) \tag{7}$$

where T is the total electron energy lost to phonon collisions (measured from the top of the p-Ge conduction band), E_g is the germanium band gap, and E_o is as defined above. For this model, a constant field is assumed.

$$F = \frac{E_g + V_B}{W_f + W_d} \tag{8}$$

where V_B is the applied reverse bias, W_d is the width of the depletion region (for a given bias), and W_f is the width of the flat band n-Ge region. The field given by this expression is an effective field which Bartelink, Moll,

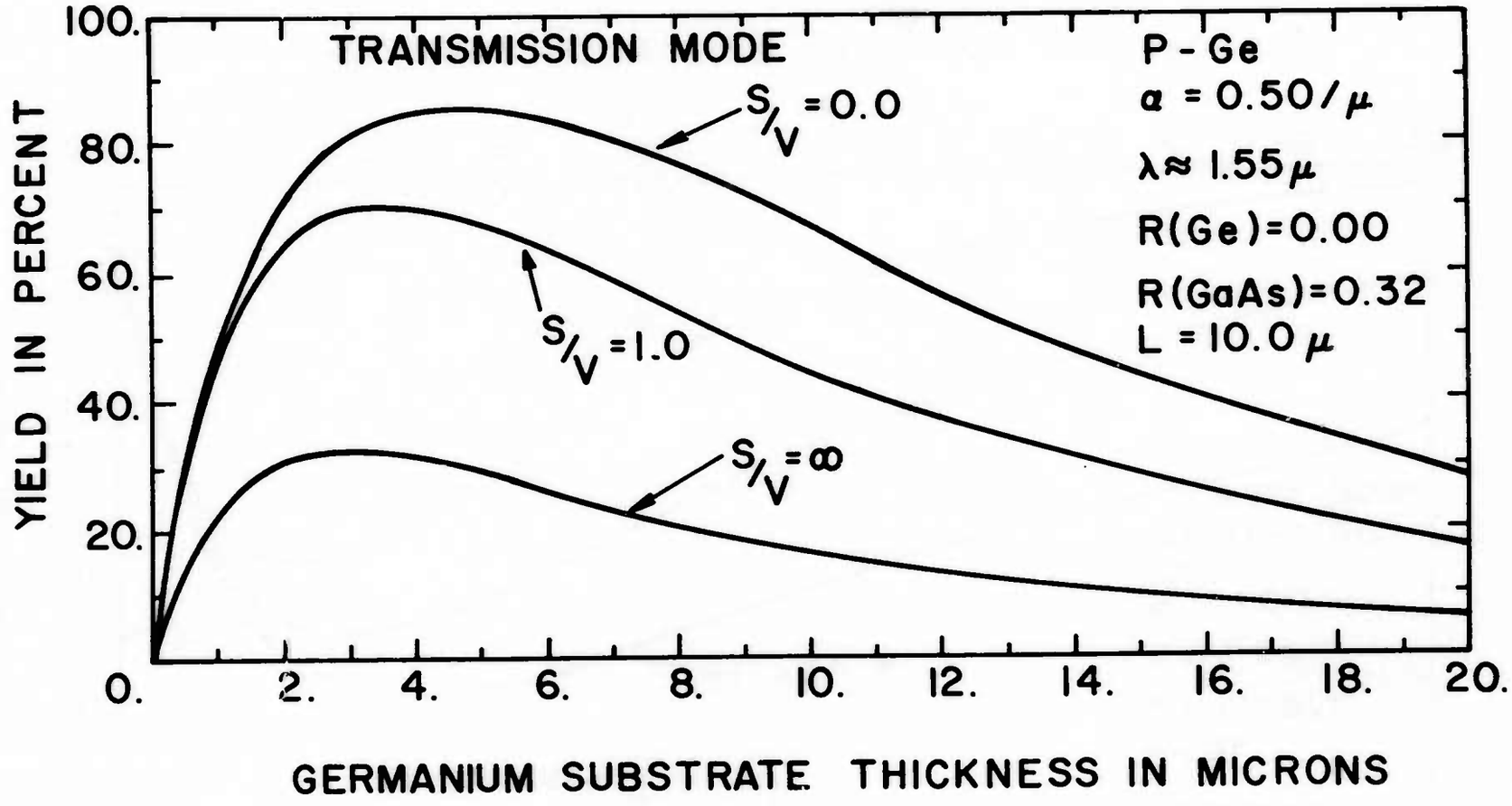

Fig. 1A. Transmission quantum yield in percent versus germanium thickness in microns for different back surface recombination velocities.

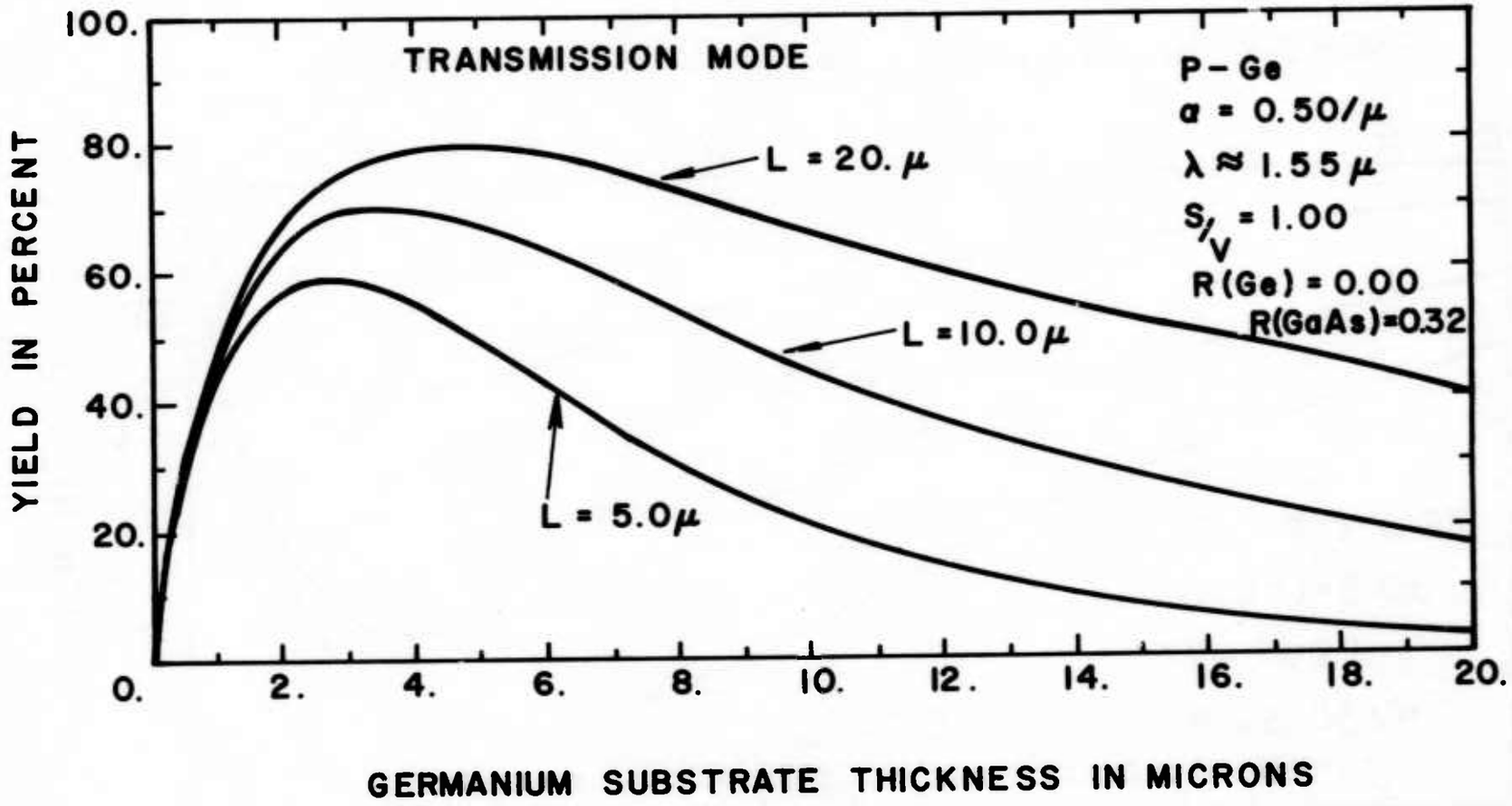

Fig. 2A. Transmission quantum yield in percent versus germanium thickness in microns for different diffusion lengths.

and Meyer have shown theoretically accounts for the transport across the n-flat-band region where there is no field. We have used the data of S. M. Sze and G. Gibbons, Appl. Phys. Letters 8, 111 (1966) which gives values for W_d at breakdown for various doping levels. These values are an over-estimate of W_d since, in operation, the junction will not be biased to breakdown. For the direct-band-gap case, we are assuming E_g = 0.8 eV, and we have assumed ℓ_p = 85 Å and E_p = .037 eV. These values are derived from data of H. Kressel and G. Kupsky, Int. J. Electron. 20, 535 (1966) which were fit to Baroff's avalanche breakdown theory, G. A. Baroff, Phys. Rev. 128, 2507 (1962). The value for ℓ_p is appropriate for a temperature of -80°C, which, as was noted before, is necessary to reduce dark current sufficiently. Inadvertently, the 0.037 eV value for E_p was not corrected for -80°C operation; the value given is for 0°K. The corrected value would be ~0.03 eV. Using the uncorrected value results in a transmission probability estimate that is on the low side.

Figure 3A is a calculated electron energy distribution plot using Eq. (7) for three different p-type doping concentrations, a fixed bias of 1.6 volts, and a flat-band n-region thickness of 250 Å. The curves are normalized so that each has the same area. The curves pertain to the energy distribution after the electrons have traversed 250 Å of n-Ge but before they have encountered the energy barrier at the n-Ge/p-emitting layer interface.

The next step is to calculate the fraction of those electrons calculated in Fig. 3A which enters the GaAs emitting layer. Bartelink, Moll, and Meyer have estimated this transmission factor; however, to utilize their results in the case where impact ionization processes are unimportant, additional approximations are required. Instead, we have taken a simpler and more direct approach involving a one-dimensional quantum mechanical transmission probability at the n-Ge-emitting layer interface. Fig. 4A shows a calculation for the 1.4 eV barrier appropriate for a GaAs emitting layer. Using this approximation, there are two factors which counteract each other to some extent in our $\ell_i/\ell_p \gg 1$ case. Fig. 3A is derived from an expression of the distribution function in spherical harmonics retaining only the first $\cos\varphi$ term. Hence, Fig. 3A shows the distribution for primarily forward-directed electrons. This leads to an over-estimate of the transmission into the GaAs. A compensating factor is that, by using the simple quantum mechanical transmission probability of Fig. 4A, we do not allow for the transmission of reflected electrons that are subsequently re-scattered in the forward direction.

Applying the quantum mechanical transmission probability to the distributions of Fig. 3A (Eq. 7) yields the distribution just inside the NEA emitting layer. Two such distributions for GaAs and InP emitting layers are shown in Fig. 5A. We have assumed a p-Ge carrier concentration of $1\times10^{18}/cm^3$, a 1.6 V bias, and a 250 Å flat-band n-region. The total transmission probability for electrons to cross the p-n junction and enter the emitting layer is given by the ratio of the areas under the curves between Figs. 5A and 3A. This involves the implicit and reasonable assumption that

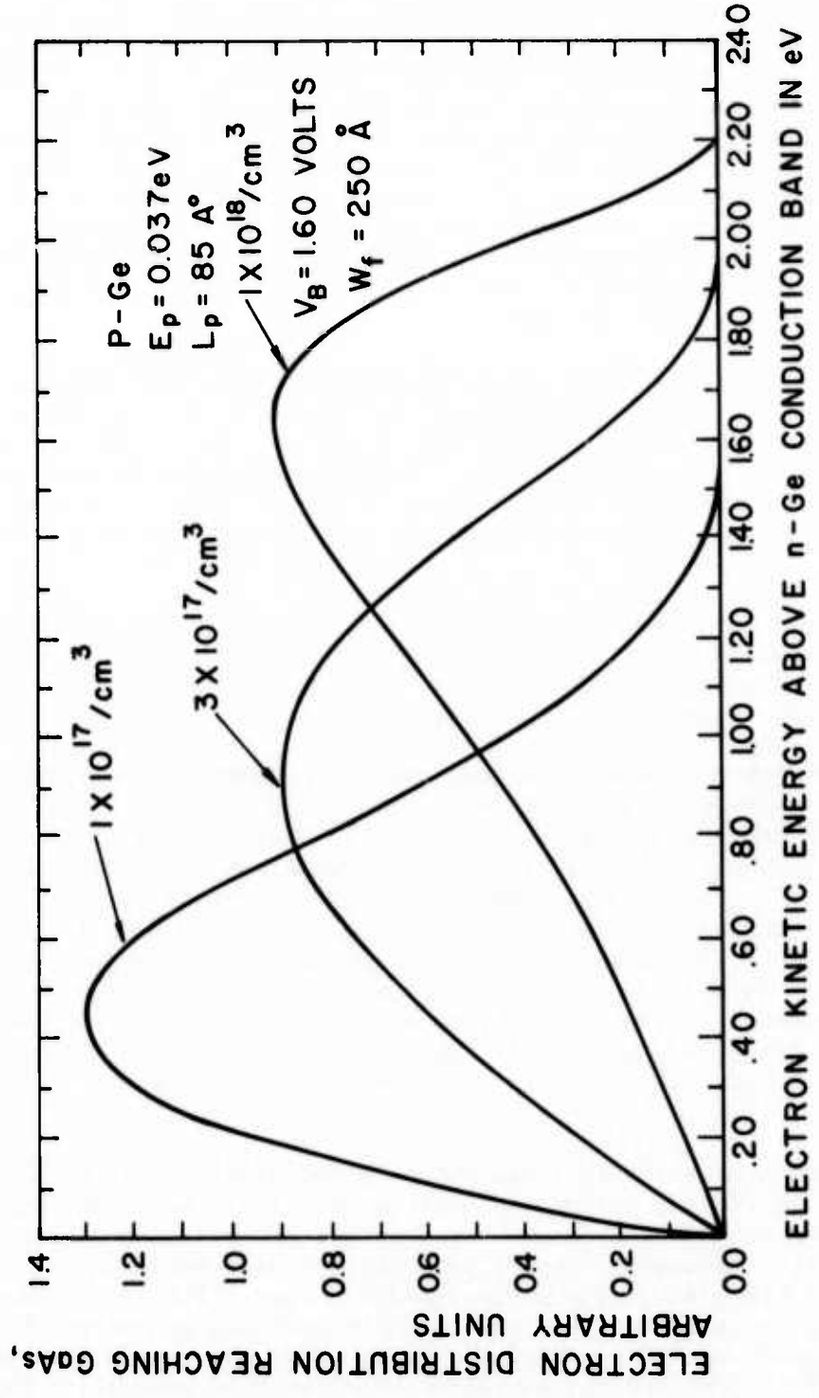

Fig. 3A. Photoelectron energy distribution reaching the n-Ge/p-GaAs interface for different germanium doping levels.

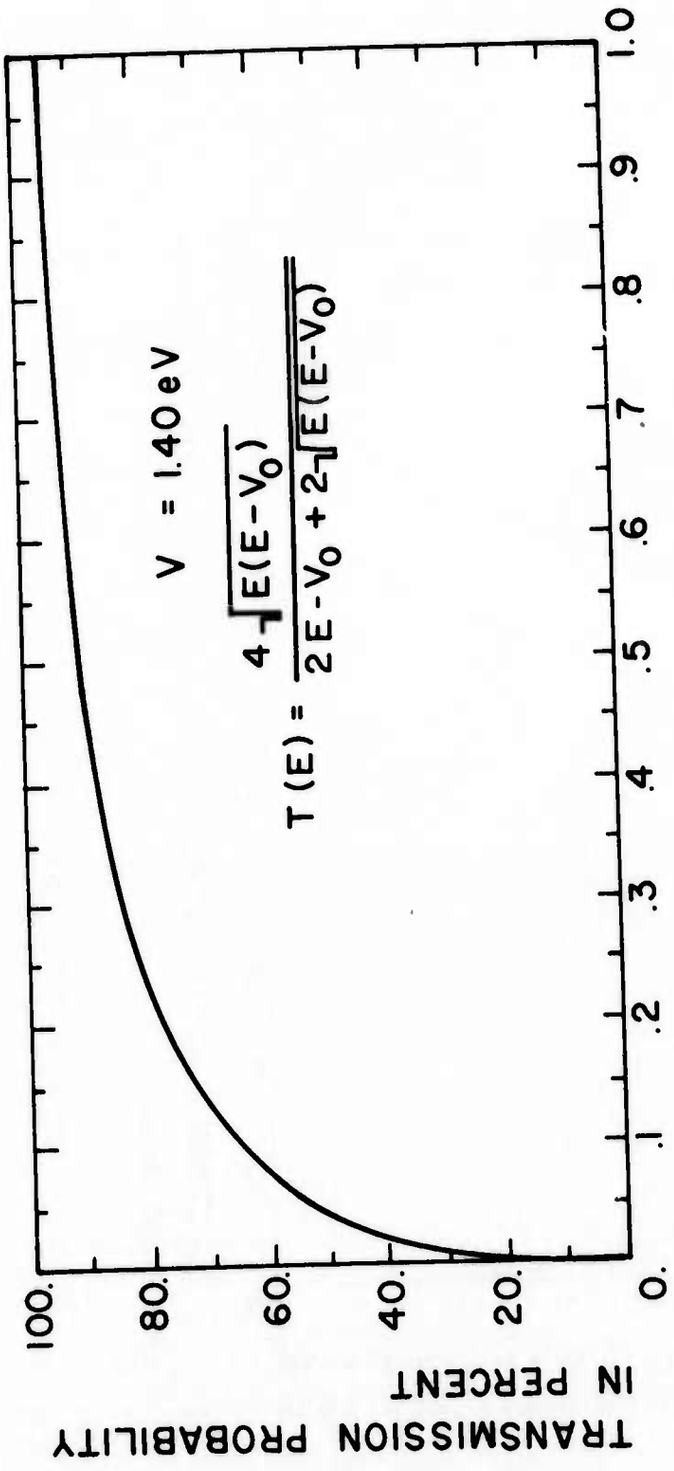

Fig. 4A. One-dimensional quantum mechanical transmission probability for a simple step potential of 1.40 eV height.

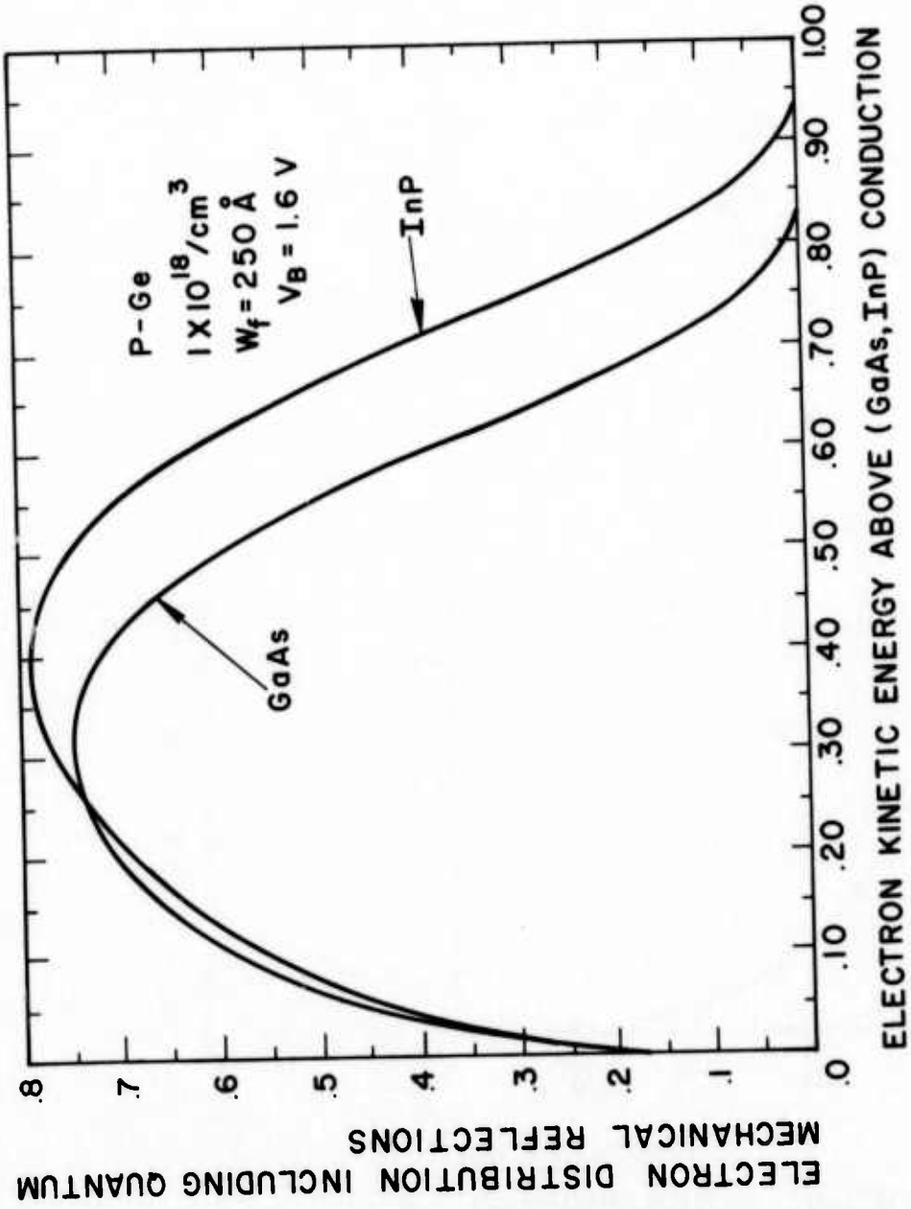

Fig. 5A. Photoelectron energy distribution incident into the emitting layer for the cases of GaAs and InP.

no electrons are lost in traversing the n-Ge layer. For the parameters used in Fig. 5A, we have a total transmission probability of 49.1% and 40.3% for InP/Ge and GaAs/Ge, respectively.

Figures 6A, 7A, and 8A give the total transmission probability versus the width of the n-region, applied bias voltage, and energy gap of the emitting layer, respectively. The results in Figs. 6A-8A do not include the quantum mechanical transmission effects. Neglecting quantum mechanical effects does not appreciably influence the parameter dependence. Transmission probabilities were obtained simply by excluding all electrons having energy below the emitting layer band gap and including all those above in these figures.

Note that, for efficient emission through the p-n junction, the width of the flat-band n-region should be ≤ 500 Å. In fabrication of this device, however, the actual width of the n-region can be somewhat larger since the junction depletion region with applied bias will extend into the n-region. The extent of the field penetration depends on the relative doping concentrations of both the p- and n-regions. A reasonable design aim, for the n-region thickness, is ~ 500 Å.

Finally, we turn to the calculation of the transmission efficiency of the emitting layer itself. This calculation utilized the same diffusion equation used for the flat-band p-Ge calculation. However, an important difference is that we have $\sim .3$-$.4$eV electrons incident on the back of the emitting layer instead of light. We assume that the resulting spatial generating function in Eq. (5) can be approximated simply by using an effective value for α, α_E. The mean range of penetration can be estimated by using the random walk equation

$$R = \lambda_p \sqrt{N} \tag{9}$$

where $\lambda_p = 85$ Å and N is the number of electron-phonon collisions before thermalizing in the conduction band of the emitter. Since $E_p = .03$ eV per collision and, from Fig. 5A, $\langle E \rangle \sim .3$-$.4$ eV, we have $N \sim 10.$ $\therefore$ $R = 85\sqrt{N} \sim 250$ Å and $\alpha_E \approx 1/R \approx 40$ μm^{-1}. We have solved the diffusion equation for $\alpha_E = 10.$, $20.$, $50.$, and $100.$ μm^{-1}, assuming that the interface can be characterized by $S/v = \infty$, since the n-Ge/GaAs or n-Ge/InP interface should be a perfect sink for electrons. The resulting yield (electrons emitted/electrons arriving in the emitting layer) versus emitting layer thickness is shown in Fig. 9A, assuming a unity NEA surface escape probability. Assuming a surface escape probability of .25-.50 gives a transmission yield of $\sim$5-15% for an emitter thickness of ~ 0.1 μm. Since $L \gg 1/\alpha_E$, the transmission yield is essentially independent of L. In fact, since $\alpha_E \cong 40$ μm^{-1}, very little is gained for $L \geq .025$ μm. Thus, the quality of the emitter need not be particularly good. Therefore, the InP/Ge system may be suitable despite lattice mismatch.

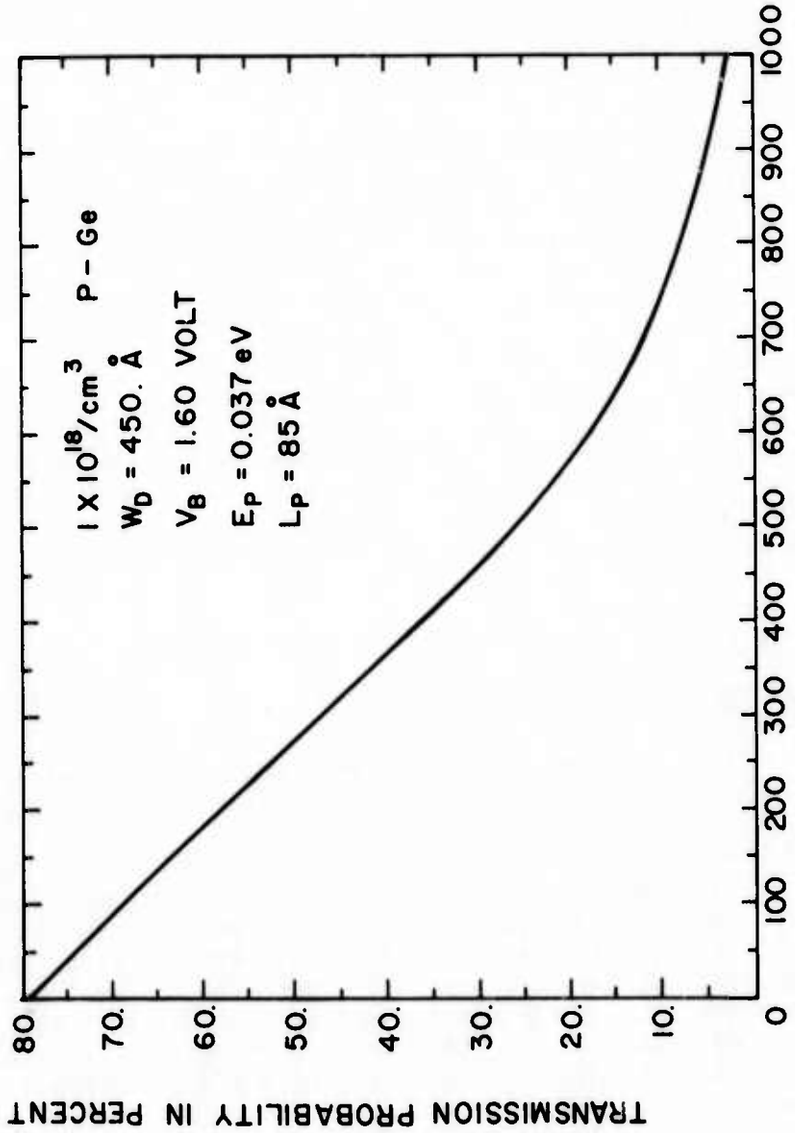

Fig. 6A. Transmission probability of photoelectrons crossing the germanium p-n junction versus n-Ge thickness for fixed bias and p-Ge doping level.

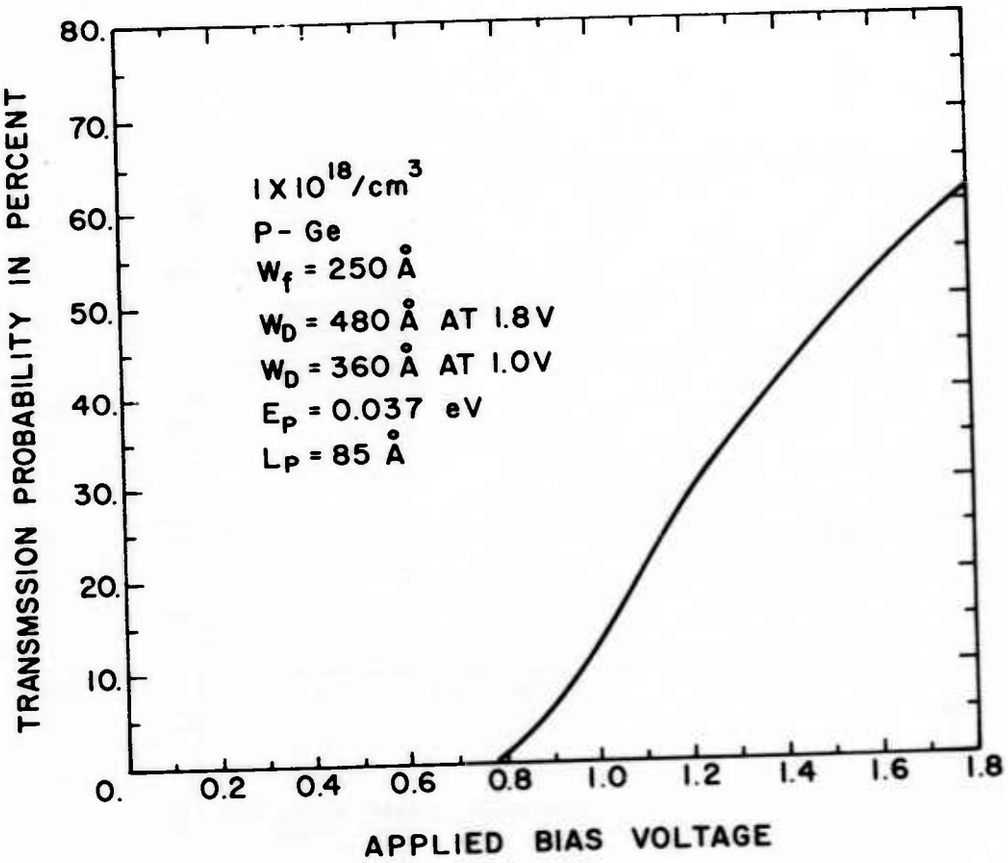

Fig. 7A. Transmission probability of photoelectrons crossing the germanium p-n junction versus applied reverse bias for fixed n-Ge thickness and p-Ge doping level.

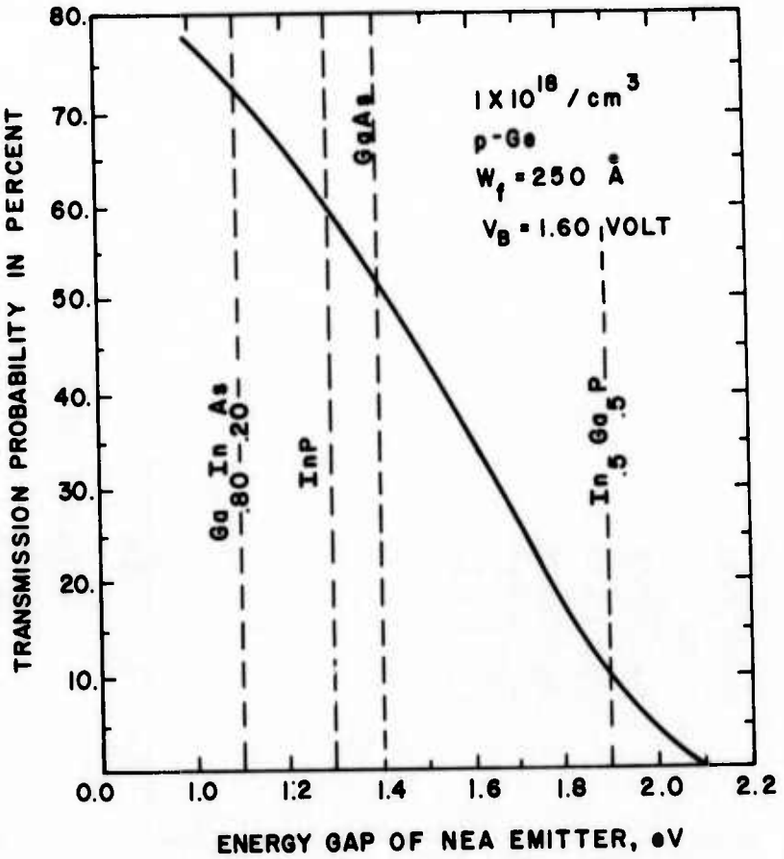

Fig. 8A. Transmission probability of photoelectrons crossing the germanium p-n junction and entering the emitting layer versus energy band gap of the emitting layer for fixed bias, n-Ge thickness, and p-Ge doping level.

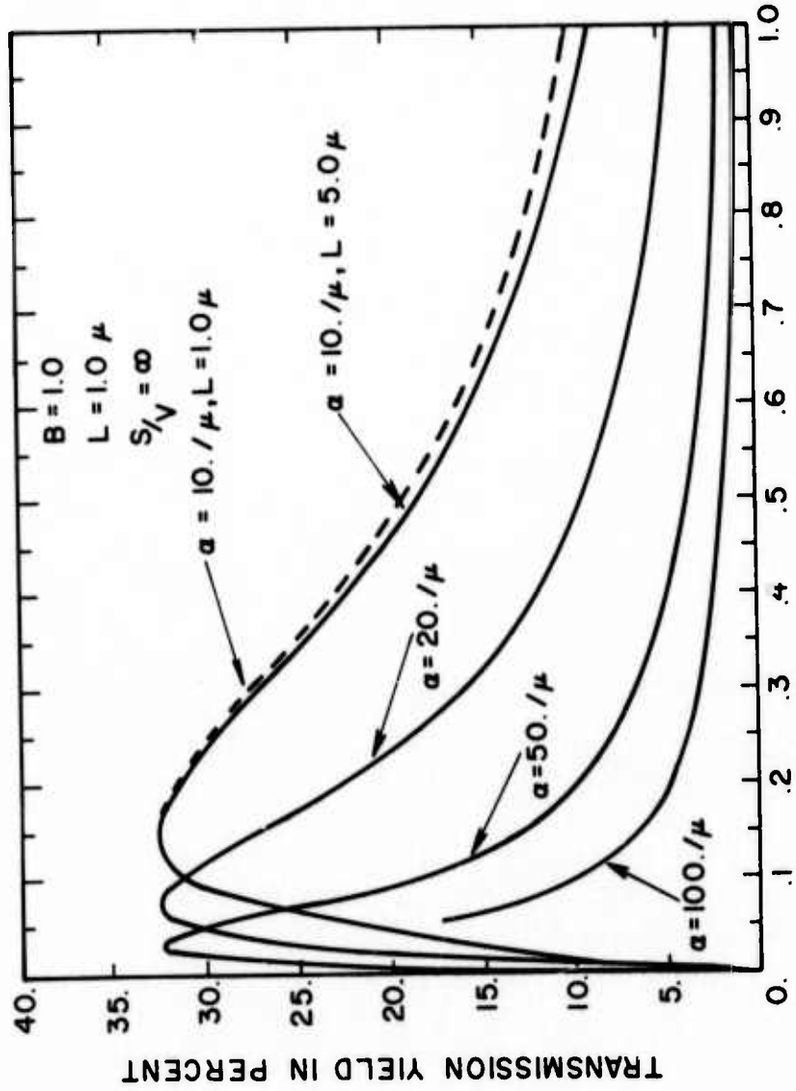

Fig. 9A. Transmission probability of electrons crossing the GaAs emitting layer versus GaAs thickness for different alpha values.

The total transmission quantum yield $Q.E._T$ of the complete device is obtained by multiplying the separate probabilities calculated. The resulting efficiency for 1.55 μm radiation is

$$Q.E._T(1.55\ \mu m) \approx (0.70)(0.40)(0.05\text{-}0.15) \tag{10}$$

or

$$Q.E._T \sim 1\%\text{-}4\% \quad . \tag{11}$$

REFERENCES

1. B. F. Williams and J. J. Tietjen, Proc. IEEE 59, 1489 (1971).

2. R. L. Bell and W. E. Spicer, Proc. IEEE 58, 1788 (1970).

3. D. G. Fisher, et al., Appl. Phys. Letters 18, 371 (1971).

4. D. G. Fisher, et al., J. Appl. Phys. 43, 3815 (1972).

5. See, for example, R. J. Hodgkinson, Solid-State Electronics 5, 269 (1962).

6. Final Technical Report, Contract No. DA44-009 AMC-1176(T), U.S. Army Engineer Research and Development Laboratories, Fort Belvoir, Va.

7. A. G. Milnes and D. L. Feucht, Appl. Phys. Letters 91, 383 (1971).

8. R. Feder and T. B. Light, J. Appl. Phys. 43, 3114 (1972).

9. D. T. Bartelink, J. L. Moll, and N. I. Meyer, Phys. Rev. 130, 972, (1963).

10. A. G. Milnes and D. L. Feucht, Heterojunctions and Metal-Semiconductor Junctions, (Academic Press, New York, 1972) p. 55.

11. J. J. Tietjen and J. A. Amick, J. Electrochem. Soc. 113, 724 (1966).

12. H. Kasano, Solid-State Electronics 16, 913 (1973).

13. C. C. Wang, Tech. Report No. ASML-TR-72-138, (1972).

14. J. J. Uebbing, J. Appl. Phys. 41, 802 (1970).

15. I. Kudman and T. Seidel, J. Appl. Phys. 33, 771 (1962).

16. H. D. Riccius and J. E. Bertie, Canadian J. Phys. 44, 1665 (1966).

17. S. M. Sze, Physics of Semiconductor Devices, (John Wiley & Sons, New York, 1969), pp. 80-83.

18. R. M. Burger and R. P. Donovan, ed., Fundamentals of Silicon Integrated Device Technology, Vol. 1, (Prentice-Hall, Inc., Englewood Cliffs, N.J., 1967).

19. F. A. Trumbore, Bell. Syst. Tech. J. 39, 205 (1960).

20. L. B. Valdes, Proc. IRE 42, 420 (1954).

21. S. M. Sze, opt. cit., p. 43.

22. S. M. Sze and G. Gibbons, Appl. Phys. Letters 8, 111 (1966).

23. W. Kern, RCA Labs., private communication.

24. W. Kern and R. C. Heim, J. Electrochem. Soc. 117, 562 (1970).

25. A. K. E. Hagopian, Chem. Phys. Letters 12, 327 (1971).

26. H. Schade, RCA Labs., private communication.

Appendix

Abrahams, M. S., private communication.

Baroff, G. A., Phys. Rev. 128, 2507 (1962).

Bartelink, D. J., Moll, J. L., and Meyer, N. I., Phys. Rev. 130, 972 (1963).

Dash, W. C. and Newman, R., Phys. Rev. 99, 1151 (1955).

Kressel, H. and Kupsky G., Int. J. Electronics 20, 535 (1966).

Schnitzler, A. D. and Malamas, J., "Image Detection and Air Glow."

Simon, R. E. and Williams, B. F., Phys. Rev. Letters 18, 485 (1967).

Sze, S. M. and Gibbons, G., Appl. Phys. Letters 8, 111 (1966).

UNCLASSIFIED
Security Classification

DOCUMENT CONTROL DATA - R & D

Security classification of title, body of abstract and indexing annotation must be entered when the overall report is classified)

1. ORIGINATING ACTIVITY (Corporate author)
RCA Electronic Components
David Sarnoff Research Center
Princeton NJ 08540

2a. REPORT SECURITY CLASSIFICATION
UNCLASSIFIED

2b. GROUP
N/A

3. REPORT TITLE
PHOTOEMISSION IN THE 1-2 Micron Range

4. DESCRIPTIVE NOTES (Type of report and inclusive dates)
Final Report 1972 April 17 - 1973 October 16

5. AUTHOR(S) (First name, middle initial, last name)
John S. Escher

6. REPORT DATE
1973 December 6

7a. TOTAL NO. OF PAGES
64

7b. NO. OF REFS
30

8a. CONTRACT OR GRANT NO
DAAK02-72-C-0412 ARPA Order No. 2182

b. PROJECT NO

d

9a. ORIGINATOR'S REPORT NUMBER(S)

9b. OTHER REPORT NO(S) (Any other numbers that may be assigned this report)
No. 4

10. DISTRIBUTION STATEMENT
Each transmittal of this document outside the agencies of the U.S. Government must have prior approval of the Director, Night Vision Laboratory, Fort Belvoir, Virginia, 22060

11. SUPPLEMENTARY NOTES

12. SPONSORING MILITARY ACTIVITY
Night Vision Laboratory
U.S. Army Electronics Command
Fort Belvoir VA 22060

13. ABSTRACT Work under this contract has focused on a field-assisted 1-2 micron-sensitive photoemitter with a reverse biased Ge p-n junction and a thin Cs-O-activated emitting layer of negative electron affinity (NEA) GaAs. The p^+-GaAs provides an effective single-crystal low-work-function large-area biasing contact for the Ge p-n junction and allows the n-Ge to be sufficiently thin for optimal performance. Calculations show that some cooling, perhaps to -80°C, will be necessary. More detailed theoretical calculations are presented which show that 1-4% quantum efficiency in transmission is possible. The optimal design parameters are calculated, and the sensitivity of the parameters is discussed. GaAs/Ge growth using the metal chloride (MC-VPE) and organometallic vapor phase epitaxy (OM-VPE) methods has been studied in some detail. Only the OM-VPE process results in a true p-GaAs/n-Ge heterojunction essential for our device. Vacuum activation levels of thick GaAs/Ge have been very high in the reflection mode - comparable to homojunction GaAs/GaAs activation levels. Ultra-thin diffused Ge junctions (less than 1000 Å deep) have been successfully fabricated using the OM-VPE method. Furthermore, NEA has been achieved on samples as thin as 0.15 micron of GaAs grown on Ge by OM-VPE. These results coupled with photovoltaic and electroluminescent measurements indicate that GaAs/Ge grown by OM-VPE should be suitable for the 1-2 micron device. Significant progress toward demonstrating the feasibility of this device has been prevented by the failure of both mesa and planar-type diodes to survive even moderate heat-cleaning cycles in vacuum. Probable breakdown mechanisms are discussed, and possible "fixes" are mentioned.

DD FORM 1473

UNCLASSIFIED
Security Classification

14 KEY WORDS	LINK A		LINK B		LINK C	
	ROLE	WT	ROLE	WT	ROLE	WT
1-2 micron photoemission Epitaxial growth of GaAs on Ge As diffusion into Ge Photovoltaic measurements on GaAs/Ge junctions						